Silicon-reduced LPCVD reaction kinetics and film morphology of molybdenum on Si surfaces
by Chang Soo Park

A thesis submitted in partial fulfillment of the requirements for the degree of Master of Science in Chemical Engineering
Montana State University

Abstract:
Molybdenum films were deposited by low pressure chemical vapor deposition (LPCVD) on (100) oriented single crystal silicon substrates by the silicon reduction of molybdenum hexafluoride (MoF6). The dependence of film thickness on deposition parameters such as temperature, total pressure, and deposition time was studied. Scanning electron microscope (SEM) and Auger electron spectroscopy (AES) were utilized to characterize the morphology of the deposited molybdenum film.

The silicon-reduced Mo films were found to be self-limiting at different thicknesses depending on the temperature and the total pressure. The film thickness at high temperatures was decreased by the severe etching, indicating the erosion of the Mo film.

The sheet resistance measurement of the films above 200 nm in thickness was found to be lower than 100 Ω/square. The film non-uniformity was also observed by measuring sheet resistance at different locations on the film, which was confirmed by SEM micrographs of the film surface.

The major impurities captured in the films were oxygen, fluorine, and carbon. The oxygen content was high when the films were not thick. High fluorine content was detected at the outermost layer of the films. This suggested that unreacted MoF6 gas or its subfluorides and decomposed fluorine atoms from adsorbed MoF6 would be the major source of fluorine at the surface.

By comparison with the literature, the findings of this study show similarities between silicon-reduced W and Mo films in aspects such as impurity content, porosity, and deposition kinetics.

SILICON-REDUCED LPCVD REACTION KINETICS AND FILM MORPHOLOGY OF MOLYBDENUM ON Si SURFACES

by

Chang Soo Park

A thesis submitted in partial fulfillment
of the requirements for the degree

of

Master of Science

in

Chemical Engineering

MONTANA STATE UNIVERSITY
Bozeman, Montana

December 1988

APPROVAL

of a thesis submitted by

Chang Soo Park

This thesis has been read by each member of the thesis committee and has been found to be satisfactory regarding content, English usage, format, citations, bibliographic style, and consistency, and is ready for submission to the College of Graduate Studies.

12-23-88
Date

Chairperson, Graduate Committee

Approved for the Major Department

12-22-88
Date

John T Sears
Head, Major Department

Approved for the College of Graduate Studies

12/23/88
Date

Harry L Parsons
Graduate Dean

STATEMENT OF PERMISSION TO USE

In presenting this thesis in partial fulfillment of the requirements for a Master's degree at Montana State University, I agree that the Library shall make it available to borrowers under rules of the Library. Brief quotations from this thesis are allowable without special permission, provided that accurate acknowledgement of source is made.

Permission for extensive quotation from or reproduction of this thesis may be granted by my major professor, or in his/her absence, by the Director of Libraries when, in the opinion of either, the proposed use of the material is for scholarly purposes. Any copying or use of the material in this thesis for financial gain shall not be allowed without my written permission.

Signature Chang Soo Park

Date Dec. 22. 1988

TABLE OF CONTENTS

LIST OF TABLES

LIST OF FIGURES

ABSTRACT

Molybdenum films were deposited by low pressure chemical vapor deposition (LPCVD) on (100) oriented single crystal silicon substrates by the silicon reduction of molybdenum hexafluoride (MoF_6). The dependence of film thickness on deposition parameters such as temperature, total pressure, and deposition time was studied. Scanning electron microscope (SEM) and Auger electron spectroscopy (AES) were utilized to characterize the morphology of the deposited molybdenum film.

The silicon-reduced Mo films were found to be self-limiting at different thicknesses depending on the temperature and the total pressure. The film thickness at high temperatures was decreased by the severe etching, indicating the erosion of the Mo film.

The sheet resistance measurement of the films above 200 nm in thickness was found to be lower than 100 Ω/square. The film non-uniformity was also observed by measuring sheet resistance at different locations on the film, which was confirmed by SEM micrographs of the film surface.

The major impurities captured in the films were oxygen, fluorine, and carbon. The oxygen content was high when the films were not thick. High fluorine content was detected at the outermost layer of the films. This suggested that unreacted MoF_6 gas or its subfluorides and decomposed fluorine atoms from adsorbed MoF_6 would be the major source of fluorine at the surface.

By comparison with the literature, the findings of this study show similarities between silicon-reduced W and Mo films in aspects such as impurity content, porosity, and deposition kinetics.

INTRODUCTION

As electronics technology moves toward the level of very large scale integration (VLSI), the requirements for the interconnect metallization become increasingly stringent. The current technology, using sputtered aluminum may well not be sufficient to meet the requirements. Step coverage, electromigration, hillocking, and eutectic formation with silicon are all serious problems of concern associated with aluminum alloy metallization. While various alloys and the introduction of diffusion barriers may alleviate some of the difficulties, the ultimate resolution of these concerns is by no means assured.

New materials for the alternative metallizations in use and under consideration in the industry are refractory metals, of which the two most commonly investigated materials are molybdenum and tungsten. These metals have much higher melting points than silicon, and their thermal expansion coefficients are similar to that of silicon. Molybdenum and tungsten are inert to both hydrofluoric acid and phosphoric acid. These properties attracted the attention of many workers in early days of large scale integration (LSI) technology [1]. Especially, chemical

vapor deposition (CVD) of these metals is an attractive process because this process can satisfy a variety of requirements for metallization, such as a diffusion barrier to prevent shallow junction spiking; low contact resistance to both n^+ and p^+ silicon; conformal step coverage of the metal (or, alternatively, a contact-refilling scheme) for planarizing vertical contacts; and contact electromigration resistance to accommodate the higher current densities in the submicron domain.

While many studies [2-10] were performed on the formation kinetics and the microstructures of CVD W films on Si by the reactions via hydrogen and silicon reduction of tungsten hexafluoride (WF_6), only a few studies [11,12] have been recently made on hydrogen-reduced Mo films by low pressure chemical vapor deposition. Furthermore, an extensive kinetic study of silicon reduction of MoF_6 has not been reported up until now. However, it is generally known that silicon reduction must take place first during Mo deposition process on account of its thermodynamic stability at the operating temperatures of CVD Mo [13]. In particular, it is important to understand the MoF_6/Si reaction because this reaction defines the contact resistance, the degree of film adhesion, and other parameters related to the metal/silicon interface.

The existing diagnostic techniques that find wide use in semiconductor applications offer great opportunities for identifying and characterizing the morphology, chemical composition, and crystallographic structure of a deposited film. These factors important in the fabrication of microelectronics are greatly affected by the deposition parameters and the rate of deposition. The study of the deposition parameters is of great importance for the realization of reliable coatings when long life operation is to be expected. The main parameters of the silicon reduction reaction in CVD are the substrate temperature and the total pressure of the metal halide and inert gas. The separate variation of these parameters have great influence on the crystal structure, the amount of impurities, and grain size, and on the number of micro bubbles that may develop under certain circumstances along the grain boundary during the reaction [14].

In this study, molybdenum was deposited on a silicon surface by silicon reduction of molybdenum hexafluoride. This was performed over a temperature range of 250-400°C and a total pressure range of 1-10 torr. The objective of this research was to study the kinetics of the silicon reduction reaction of molybdenum hexafluoride on a Si surface and investigate the dependence of the impurity concentration and

the film morphology on the deposition parameters. An acid dissolution method was utilized to measure the amount of the Mo film deposited. The film morphology and the impurities' contents were investigated by the modern surface science techniques: scanning electron microscopy (SEM), and Auger electron spectroscopy (AES).

BACKGROUND

New Metals for Metallization

Very large scale integration (VLSI) and the continued evolution of smaller and smaller devices has aroused concern about the existing metallization schemes and interest in the development of new metallization schemes for gates, interconnections, and ohmic contacts, and has motivated continued study of the reliability of aluminum and its alloys as current carriers.

The applicability of any metallization scheme in VLSI depends on several requirements such as low resistivity, good adherence, stability throughout processing, and good device characteristics and lifetimes. Most important of these requirements are the stability of the metallization throughout the integrated circuit (IC) fabrication process and its reliability during the actual use of the devices [15].

In the semiconductor industry, aluminum is a well known and important metal. This metal is most widely used for metallization of silicon devices such as contacts and interconnects in the VLSI devices due to its low room temperature resistivity and excellent adhesion to SiO_2. However, aluminum has a relatively low melting point

(660^0C), and upon approaching this temperature the transfer of momentum from electrons is increased, causing transport or migration of the conductive material. This electromigration is a potential source of breakdown in aluminum interconnect lines. Also, good step coverage is hard to achieve with aluminum because at the present time physical vapor deposition is the only method available for depositing aluminum. It is very difficult to get the proper alloy composition to prevent junction spiking and electromigration as well. Particulate interface, hillock formation and etching difficulty are also other problems which may be encountered during processing.

On account of a rapid growth in the semiconductor industry of today, this competitive condition brings about the need for a new metal with the capabilities of making smaller, less expensive, and more productive components for integrated circuits. The problems brought about by using aluminum have also accelerated the need for a potential new contact metal such as refractory metals of molybdenum, tungsten, and tantalum. Recently, molybdenum has shown potential applications not only as a contact or interconnect, but in other areas as well. For example, molybdenum has been used for diffusion or corrosion barriers due to its high ductility, and for parts with complex shape.

There has also been considerable interest in molybdenum as a gate electrode for VLSI fabrication.

Molybdenum could be an excellent interconnecting metal because it can be selectively deposited on silicon; no deposit occurs on the SiO_2 layers [16-18]. Therefore, the number of process steps can be reduced by eliminating lithography that is the process of transferring geometric shapes on a mask to the surface of a silicon wafer. If the selective molybdenum deposition process is proven reliable and reproducible, this process will probably be the best for multilevel structures as well as for contact metallization.

Reactors for Chemical Vapor Deposition (CVD) of Mo and W

The first distinction between reactor types is whether they are hot-wall or cold-wall reactors, and this is dependent on the method used to heat the wafers. When radiant heating from resistance-heated coils surrounding the reaction tube is utilized, not only the wafers but also the reaction chamber walls become hot, and hence such designs are known as hot-wall reactors. In these systems, film forming reactions (and as a result, film deposition) occurs on reaction chamber walls as well as on substrates. If

the energy source is mounted within the reactor to primarily heat the wafers and susceptor, and not to cause appreciable heating of the reaction chamber walls, systems heated by this method are termed cold-wall reactors. In some cold-wall systems, however, significant chamber wall heating can still take place, and provisions for cooling the walls must be implemented (e.g. by water cooling) to prevent reactions or depositions from occurring there [19].

The next criterion used to distinguish reactor types is their pressure regime of operation (atmospheric pressure or reduced pressure reactors). Atmospheric pressure CVD reactors (APCVD) were the first to be used by microelectronics industry [20,21]. Hence, most CVD refractory metals' work for VLSI in early days was done in cold-wall reactors operating at atmospheric pressure since operation at atmospheric pressures kept reactor design simple and allowed high film-deposition rates. APCVD, however, is susceptible to gas phase reactions, and the films typically exhibit poor step coverage. Currently, atmospheric reactors are primarily used for low-temperature oxide (LTO) deposition and epitaxy.

Low pressure chemical vapor deposition (LPCVD) in some cases is able to overcome the uniformity, step coverage, and particulate contamination limitations of early APCVD systems

[22-24]. By operating at medium vacuum (0.25-2.0 torr), and higher temperatures (550-600°C), LPCVD reactors typically deposit films in the reaction-rate limited regime, since at reduced pressure the diffusivity of the reactant gas molecules is sufficiently increased so that mass-transfer to the substrate no longer limits the growth rate. The elimination of mass-transfer constraints in reactor design increases the wafer throughput capacity of the reactor. Low pressure operation also decreases gas phase reactions, making LPCVD films less subject to particulate contamination. LPCVD is used for depositing many types of films, including Mo, W, poly-Si, Si_3N_4, and SiO_2 [19]. Especially, LPCVD of tungsten is currently under intense investigation for its potential application in VLSI circuits. Applications investigated include shunting of polycrystalline silicon gate and interconnect lines of tungsten and molybdenum films with a lower resistivity to reduce the resistance and capacitance (RC) time constant [25,26] associated with interconnection paths, formation of a barrier between silicon and aluminum to reduce aluminum spike-induced failures [26,27], planarization of the multilevel interconnect process [27,28], low resistance contact formation to drain and source regions [25,27], and formation of a Shottky barrier p-channel metal oxide silicon

(MOS) transistor to form latch up-free complimentary metal oxide silicon (CMOS) [27].

Plasma-assisted depositions provide films at very low sample temperatures. They do this by reacting the gases in a glow discharge, which supplies much of the energy for the reaction. Although the electron temperature in the discharge may be near 10^{5}°C, the sample temperature is between 100 and 400°C. By using this technique, a large number of inorganic and organic materials have been deposited but only two are useful in VLSI technology: plasma deposited silicon nitride (SiN) and plasma-deposited silicon dioxide [29]. Due to undesirable incorporation of the impurities such as hydrogen, nitrogen, and oxygen, this technique is not useful for high purity deposition of thin metal films necessary for VLSI fabrication.

As described earlier, molybdenum and tungsten were most commonly investigated for VLSI technology. These metals can be patterned to serve as diffusion masks [29]. LPCVD of molybdenum, especially, provides several advantages over aluminum besides those of molybdenum stemming from high melting temperature (2610°C), high corrosion resistance, low resistivity, and an expansion coefficient that is close to that of silicon. The attractiveness of LPCVD of Mo for metallization comes from the conformal nature of coating

(i.e., good step coverage), the ability to coat large numbers of substrates at a time, the relatively simple equipment, and higher purity deposits. If the attractiveness is proven by further research, low interconnect resistance and a high operating speed can routinely be obtained by using LPCVD of Mo.

Reaction Schemes of Film Deposition (Mo,W)

The chemical vapor deposition of Mo on Si, using MoF_6 as the source, can involve two reactions. The first reaction, the Si reduction of MoF_6, also known as the displacement reaction, involves consumption of Si:

$$2MoF_6\ (g) + 3Si\ (s) \text{ ------> } 2Mo\ (s) + 3SiF_4\ (g)$$

where (g) and (s) are gas and solid phases, respectively. Even when hydrogen is present, this reaction will always occur first. Thicker Mo films can be grown on the Si-reduced Mo film by H_2 reduction of MoF_6 according to a second reaction:

$$MoF_6\ (g) + 3H_2\ (g) \text{ ------> } Mo\ (s) + 6HF\ (g)$$

It is generally believed that molybdenum and tungsten chemistry is similar enough to expect similar CVD behavior. Kinetic work by Broadbent and Ramiller [5] and Sahin et al. [11] showed that deposition of tungsten from WF_6 was very similar to molybdenum deposition from MoF_6. Free energy

changes shown in Table 1 indicate that both MoF_6 reactions are thermodynamically possible [13] and the silicon reduction is more favorable.

Table 1. Free Energy Changes for MoF_6 Reactions to Form Mo

Temp.	ΔG^o (kcal/mol) H_2 Reduction	ΔG^o (kcal/mol) Si Reduction
400°C	-50	-213

Although the great majority of CVD Mo films for IC applications are deposited by H_2 reduction, it is important to emphasize that the displacement reaction will always take place first. Therefore, it is the Si reduction reaction that determines the nature of the Mo/Si interface. This interface will determine such important device characteristics as contact resistance and leakage current, and such physical characteristics as interfacial smoothness and silicide formation kinetics [6].

Si Reduction of MoF_6 and WF_6

In order to achieve good contact between silicon and metal a clean interface is essential. In the case of CVD

selective tungsten deposition the cleanliness of the interface is attributed to the initial phase of the deposition by silicon reduction of WF_6. During that phase only 100-200Å are consumed while leaving a clean silicon surface, which makes good contact with the deposited metal. The tungsten deposited inside the contacts can be used as a contact barrier to protect underlying junctions from aluminum spiking and improve the electromigration resistance of the contacts [30].

This reaction deposits a thin layer of tungsten while consuming some of the exposed silicon. This reaction stops after tungsten film continuity is achieved, which is known as the self-limiting, as it acts as a physical diffusion barrier between the silicon and the WF_6. While many researchers have agreed with this phenomena, there still exist some discrepancies among the results published by now. For instance, in a study by McConica and Krishnamani [31] the thickness was found to be self-limiting in every case, and independent of time, temperature, and partial pressure of WF_6. The experiments were carried out for temperatures ranging from 250 to 375°C and partial pressures of WF_6 ranging from 66 to 664 Pa. The deposition time was varied from 1 to 20 minutes. Moriya and Itoh [32] also carried out the silicon reduction reaction in a low pressure region

of 0.1-0.2 torr for a temperature range of 150-600°C. However, they reported that the W films self-limited at different thicknesses, depending on the substrate material and the deposition parameters; the deposition temperature, the partial pressure of WF_6, and the total pressure.

Conventional wisdom in the CVD W deposition has stated many times that the Si displacement reaction results in thin (~10nm), self-limiting films of W. However, Tsao et al. [10] have seen silicon-reduced W films as thick as ~200nm and Mianowski et al. [33] have seen similar films up to 800nm thick in a linear relation with the deposition time when deposited in N_2 ambient gas at atmospheric pressure. An unusual temperature dependence of W film growth by Si reduction was also reported by Green et al. [6]. According to their results, films deposited below 310°C self-limit at about 6nm of full dense W. In a temperature range of 320 to 450°C, film thicknesses up to ~95nm were observed. In the higher temperature range, 500 to 700°C, film thicknesses of about 200 Å were observed. This type of unusual decrease in thickness may result from a slow etching of the films (~0.4nm/min) by WF_6 [10]. To explain the temperature dependence and the self-limiting behavior of film growth (regardless of the ultimate film thickness at which the film self-limits), it was proposed that the rate-controlling step

would be a surface-catalyzed reaction. Thus, the temperature dependence of the sticking coefficient of a reactive intermediate probably controls the reaction.

The microstructures were studied for silicon-reduced W films deposited between 210 and 700°C [6]. In this study it was observed that the silicon-reduced W films were porous and discontinuous, and each grain was composed of tiny particles separated by a fine pore network. The grains were therefore "spongy", and reminiscent of a partially sintered mass of particles. Especially, the percentage of space occupied by trapped gases, pores, and inclusions in the CVD W films, ranging from 40 to 58.8%, accounts for the reduced density of the deposited films than that of bulk tungsten.

The impurity content obtained from Auger depth analysis by Tracy [8] showed that oxygen, fluorine, and carbon impurities were low; the profiles also indicated that most oxygen laid at the Si/W interface. The oxygen percentage in the silicon-reduced films obtained from XPS(X-ray Photoelctron Spectroscopy) analysis was found to be up to ~30% [31]. The microstructure of the deposited layer was found to be similar with surface oxide characteristics [10,34] since some oxygen in the native oxide layer on the silicon surface may incorporate during film formation.

Kinetic data on the silicon reduction of molybdenum hexafluoride is rare. In a few studies it was reported that the Mo film growth via the silicon reduction does not self-limit at all and furthermore the rate of reaction with silicon was very high. A kinetic data by Lifshitz et al. [35] showed that molybdenum films grew linearly with time with high deposition rate (~100nm/min), whereas tungsten ceases growth after the deposition of a relatively thin film. Woodruff and Sanchez-Martinez [12] also observed very thick films of molybdenum (up to 9.2 microns) for just the MoF_6/Si reaction. An interesting feature reported in the study [35] was the incubation time that precedes deposition. This incubation time was shorter for higher deposition temperatures and for hydrogen containing reactant gas streams. Clearly, the deposition rates strongly depend on temperature. According to the results the films formed at 250°C were an order of magnitude thicker than the films deposited at 200°C.

As stated earlier, the kinetic data on LPCVD molybdenum from the silicon reduction of MoF_6 is very limited because there has been no comprehensive and independent study on the kinetics. Studies by Woodruff and Sanchez-Martinez [12], and Lifshitz et al. [49] only included brief kinetic data of the silicon reduction reaction.

Despite the difference in the growth kinetics between Mo and W films, the morphology of Mo and W films exhibited many common features. First, it was reported that the films deposited over silicon were porous, separated in some cases at the grain boundaries, and had a high oxygen content distributed uniformly through the film, resulting in a high sheet resistance [35]. It is generally believed that such porosity of the films allows reactants and products to move freely to and from the silicon/metal interface, and the amount of the oxygen in the films depends on the temperatures at which the reactor was opened to air.

Second, it was reported that the metal-silicon interfaces look similar, with characteristic protrusions densely covering the interface [36]. Especially, these protrusions were considered to be the precursors of "tunnel effect", or "wormholes", which have been observed mainly in hydrogen-reduced W films [9,37,38], and in silicon-reduced Mo films [39].

Hydrogen Reduction of MoF_6

The information on CVD molybdenum from MoF_6 is so limited because in the early days much more work was carried out for CVD of Mo from the chloride [40-43] and from the carbonyl [44,45]. The primary concern of most of these

studies was to investigate possible uses of molybdenum in the production of various electronic components. In addition, these two compounds were reported to be inadequate for a molybdenum source in the VLSI fabrication process because the literature on carbonyl showed the incorporation of too much carbon in the films and the disadvantage in using $MoCl_5$ is that at low temperatures below 150°C the chlorides condense on any surface.

Similar to the kinetics of the H_2 reduction of WF_6, the kinetics of the H_2 reduction of MoF_6 showed the rate of molybdenum deposition to be a square root dependence on the hydrogen partial pressure and no dependence on the MoF_6 partial pressure over a temperature range of 250-350°C and a total pressure range of 0.9-10.0 torr [46]. From an Arrhenius plot for reciprocal temperature versus r (rate of deposition) for total pressure of 0.9 and 5.0 torr and for total deposition times of five and ten minutes, an average activation energy was determined to be 76,000 J/mol. A statistical average of the values of all the preexponential factors was calculated to be 2.02×10^6 nm/s $torr^{-0.5}$.

In a study by Shroff [47], the molybdenum films were deposited at temperatures of 600 to 1300°C and at pressure of 0.01 to 760 torr on various substrates such as copper, stainless steel, and molybdenum. The influence of the

pressure on the deposition characteristics of molybdenum and tungsten was found to be similar. They suggested that the mechanism of the growth was due to the combined effect of the pressure and the temperature. In the case of Mo at low temperature and low pressure in the early stages of the reaction there was a slight etching of the base material, especially when it was molybdenum by the molybdenum hexafluoride or its decomposed sub-products.

The molybdenum film characteristics are also dependent on the deposition conditions. Sahin et al. [11] reported a significant amount of oxygen, fluorine, and carbon in the molybdenum films. A study by Woodruff and Sanchez-Martinez [12] was performed to investigate the quality of CVD Mo film from MoF_6 at low temperatures and pressures. They observed that the films deposited over silicon are porous and have a high oxygen content. In particular, it was shown that the Mo-Si interface was rough, indicating that Si reduction reaction took place.

In a study by Chen et al. [48], polycrystalline molybdenum films, 500Å in thickness and 50-150nm in grain size, were chemical vapor deposited on (100) oriented, n-type silicon substrate heated to 650-700°C in hydrogen ambient. Ion beam-induced interfacial reactions in molybdenum thin films were investigated using transmission

electron microscopy (TEM), with which they found hexagonal $MoSi_2$, tetragonal $MoSi_2$, and hexagonal $MoSi_3$, mainly formed along grain boundaries. This was also found by in-situ annealing of the thin foil at 700°C for 2h in the electron microscope. They concluded that the observations may provide direct evidence of the important role of grain boundary diffusion in the formation of silicides.

Hydrogen Reduction of WF_6

Many studies have been performed to investigate the kinetics of the hydrogen reduction of tungsten hexafluoride at various temperatures and pressures. It was shown that the growth rate at a given temperature displayed a square root dependence on changes in either the total pressure or the hydrogen partial pressure and no dependence on changes in the WF_6 partial pressure [5,7,49,50]. The activation energy was found to be 69,000 J/mol (0.71eV) on both a Si substrate [5] and a W substrate [49].

The characterization of a deposited film requires the use of a variety of diagnostic techniques. Modern surface science and other techniques provide the capability of studying metal films designed for use in microelectronics. These techniques allow the researcher to investigate such things as the uniformity and purity throughout films, the

porosity of a deposited film, and the condition of the interface after the deposition of a metal on a surface. This film morphology is greatly affected by the deposition parameters and the rate of deposition.

A few studies have been reported on the film morphology and chemical composition of the hydrogen-reduced W films. There exist at the tungsten/silicon interface a number of morphological features which occur on a submicron to atomic level. Paine et al. [9] reported the common features such as the formation of wormholes in the silicon substrate, tungsten/silicon interfacial roughness, and lateral encroachment of tungsten beneath silicon/silicon dioxide interfaces. It was also emphasized that the physical properties of the initial 10 nm of tungsten would play a role in interface morphology development.

In a study by Shroff and Delval [14], tungsten was deposited from the vapor phase by the reduction of WF_6 by hydrogen on various substrates such as copper, stainless steel, and molybdenum. The deposition temperature ranged from 450-1200°C. The reaction was carried out at partial pressures of 5-760 torr; and the hydrogen to hexafluoride ratio was varied from 1 to 60. Their structural study of the deposits with optical and scanning microscopes showed that the number of very small voids or bubbles in the

deposits tended to increase with increasing H_2/WF_6 ratio and pressure, and decreased with increasing deposition temperature. The amount of gaseous fluorine impurity measured by the activation process, showed that the higher the ratio, the higher was the percentage of samples with low F content.

The characterization study of CVD W by MacLaury et al. [51] was performed at 300°C with a 30/1 H_2/WF_6 flow ratio at 0.3 torr. In the study it was found from SIMS(Secondary Ion Mass Spectrometer) analysis that fluorine was a major contaminant. The transmission electron microscopy (TEM) results indicated that some kind of damage to the (100) Si/SiO_2 interface in the form of worm tracks in the silicon under the SiO_2 step. The transmission electron micrographs published by Stacy et al. [52] support the fact that during the tungsten deposition filaments (variously called "wormholes" or "tunnels") were formed in the silicon substrate. However, filament growth was not observed onto aluminum but onto silicon. These observations led Stacy et al. [52] to conclude that the vaporization of silicon by fluorinated species was involved.

Scanning Electron Microscopy (SEM)

The morphology of the Mo films deposited can be determined by scanning electron microscopy, which has become an important tool for VLSI analysis because it has the capability of providing much higher magnification, resolution, and depth of field than optical microscopy [53]. That is, the resolution of SEM can be up to 1nm (100nm is routinely obtained), the magnification from 10X-100,000X and the depth of fields of 2-4 μm at 10,000X. Especially, the high depth of field makes SEM useful for high magnification (i.e. >2,000X) examination of film thickness below 1 μm [54]. SEM analysis yields information on linewidth, film thickness, step coverage, interface roughness, and other morphological data.

In the scanning electron microscopy, an electron gun, usually consisting of tungsten or LaB_6, is used to create a beam of electrons that is accelerated to energies of 500eV-40keV, focused to a small diameter, and rastered across the sample surface. The electrons striking the surface produce three useful types of radiation: x-rays, secondary electrons, and backscattered electrons. A large fraction of the electron spectrum (usually below 50eV) are secondary electrons, which are produced by inelastic collisions of the primary beam and the inner shell electrons of the sample

atoms. Because they posses such low energies, only secondary electrons created close to the surface actually escape and are detected. The detected electron current, which can be due to secondary or backscattered electrons, but is typically the former, is used to modulate the intensity of an electron beam in a cathode ray tube (CRT). The CRT beam produces an image of the sample surface whose contrast is determined by variations in the secondary or backscattered electron flux [55].

Auger Electron Spectroscopy (AES)

Auger electron spectroscopy has emerged as one of the most important techniques for determining the elemental composition of CVD films qualitatively and quantitatively. The utility and popularity of AES is based on its high sensitivity, its excellent elemental selectivity for all atoms except H and He, the availability of energy analyzers with high transmission, and the good lateral resolution afforded by electron beam excitation.

This technique is based on the fact that each element of the periodic table will, when excited by the ionization of a core level, emit Auger electrons at characteristic energies that are usually only slightly influenced by chemical environment. In the precursor process to the

Auger emission the initial core hole is produced by electron impact ionization in which the atom undergoes the transmission

$$A \text{ -----> } A^{+}(i) + e^{-}$$

Here the notation $A^{+}(i)$ indicates that the hole in A is in level i. The Auger process may then be written

$$A^{+}(i) \text{ -----> } A^{2+}(j,k) + e^{-}$$

where the emitted electron e^{-} has kinetic energy E_k outside the solid; that is, it lies at a level $E_k + \Gamma_s$ above the Fermi level, and the atom is left doubly ionized with holes in its j and k levels. This process may be understood as involving an electron from an outer level j (or k), which is ejected. This simple explanation, however, neglects final-state interactions.

AES can be used to conduct a depth profiling of the deposited molybdenum. By combining continuous sputter etching with AES, the composition as a function of depth into the surface can be determined. This method has been extensively applied to a variety of technologically important problems in semiconductor, metallurgy, and thin-film processing [56]. A difficulty from this technique comes from the case in which quantitative data is needed. In that case, usually a standard is also required. That is, a sample containing a known quantity of the substance

whose presence is being quantitatively identified (determined with confidence by an alternate diagnostic technique), must be analyzed to establish reference signal magnitudes for the characterization technique being used. In fact, all compositional analysis techniques except Rutherford backscattering (RBS) require such standards as a prerequisite to obtaining accurate quantitative data.

RESEARCH OBJECTIVES

The objectives of this study are basically two-fold:

1. Study the kinetics of the silicon reduction of molybdenum hexafluoride on a silicon surface.

2. Characterize the silicon-reduced Mo films by AES, SEM, and and compare the findings with those reported in the literature.

EXPERIMENTAL EQUIPMENT

The reactor for LPCVD Mo used in this study was drawn in Figure 1, which was divided by function into the following primary components: the gas flow controller, the reactor and heater, the chamber pressure controller, the pumps, and the after-burner and alumina trap.

Gas Flow Controller

Electronic E-1 grade pure helium (99.9995%, Scientific gas products inc.) and molybdenum hexafluoride (99.9% pure, SERAC Co.) were introduced into the reaction chamber by MKS type 1259 controllers, which were connected to a MKS 247B four channel readout and power supply unit. The flow rates of both He and MoF_6 gases could be set at 3 and 9 sccm, respectively. The controllable gas flow ranges were 0-145 sccm for helium and 0-21 sccm for molybdenum hexafluoride.

Reactor and Heater

The 6 way-cross stainless steel reaction chamber was wrapped with fiberglass heating tape to reduce water vapor inside the reactor. The substrate heater was mounted on the stainless steel rod attached to a flange. A 5cm x

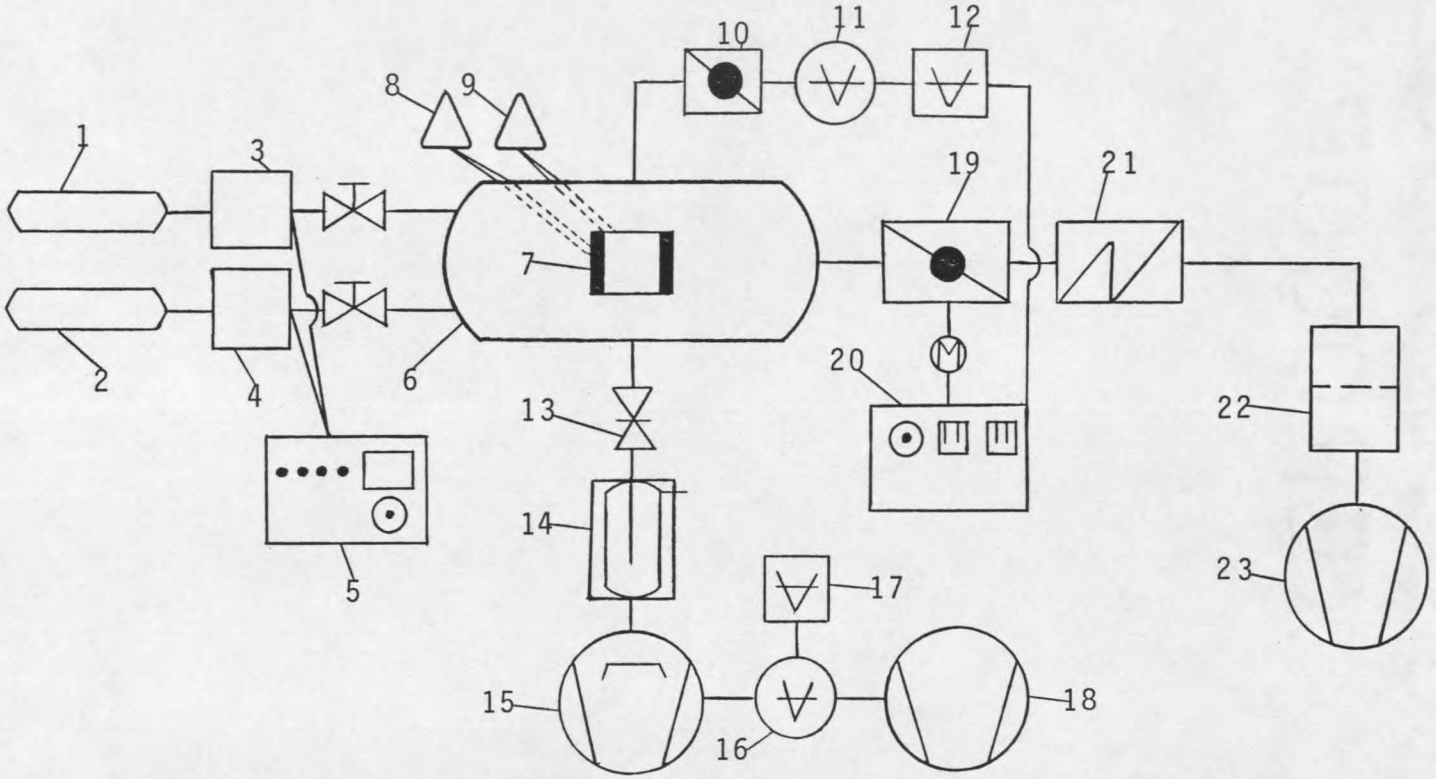

1,2 He & MoF_6 gas cylinders
3,4 Gas flow controllers
5 247B 4 channel readout
6 6-way cross vacuum chamber
7 Substrate heater
8 Digital thermometer
9 Substrate power supply
10 Butterfly valve
11 Baratron 127A gauge
12 PDR-D-1 digital readout
13 Gate valve
14 Liquid nitrogen trap
15 Diffusion pump
16,17 Forepressure gauge & power supply
18 Roughing pump
19,20 Exhaust valve & controller
21 After-burner
22 Alumina trap
23 Varian roughing pump

Figure 1. Molybdenum LPCVD System

3.5cm x 2.5cm stainless cell block was used as the substrate holder and heating unit. Four ceramic tubes with Ni-chrome wire running through them in series were equally placed through holes made in the block to prevent a thermal gradient (e.g., a uniform heating distribution) of the substrate. The total resistance of the wires was about 2.7 ohms.

The wires were spot-welded to tantalum rod connected to copper feed-throughs welded in the access flange. These feed-throughs were in turn connected to a variac power supply. The maximum temperature that could be obtained by resistive heating of the wires was up to 450°C due to the relatively low total resistance of the wires.

Two 1/4" stainless steel rods which were screwed into the feed-through flange acted as the support for the substrate holder. The underside of the substrate holder had two machined grooves for positioning the holder on the rods. The substrate holder was spot-welded to the rods.

An alumel-chromel thermocouple was spotwelded to the center of the sample holder. The thermocouple wires were attached to larger diameter alumel-chromel feed-throughs which were added in the access flange. The temperature was recorded by a digital thermometer.

Pressure Controller

A MKS throttle valve type 253-1-40-1 was clamped to the reaction chamber. The chamber pressure was automatically controlled by regulating the valve opening (e.g., the pumping speed) by a MKS exhaust valve controller type 253A. The chamber pressure was measured by an absolute capacitance manometer gauge, MKS baratron type 127A, which was mounted on top of the reaction chamber. The pressure was displayed on a MKS power supply and digital readout PDR-D-1.

Pumps

The pumping system consisted of a diffusion pump and two mechanical roughing pumps.

The diffusion pump (CVC-M60) was attached to the bottom of the liquid nitrogen trap which prohibited backstreaming arising from evaporation of oil from the top jet. Evacuation of the reaction chamber by the diffusion pump was started by opening a gate valve (model SVB-2.5V14, Torr vacuum products inc.) which was placed between the reaction chamber and the liquid nitrogen trap. Also, low vapor pressure pump fluid was used to minimize the backstreaming. The chamber pressure obtainable with this pump was up to 10^{-7} torr. Attached to the diffusion pump outlet was a Welch roughing pump with a pumping capacity of 25 1/min.

The other roughing pump was a Varian SD-300. This pump has a maximum speed of 300 l/min and was used to exhaust the residual reaction gases. All of these roughing pumps were placed in an exhaust hood.

After-Burner and Alumina Trap

After-burner and alumina trap made of a stainless steel were located in order between the exhaust valve and the roughing pump in the hood. The after-burner was filled with stainless steel shavings and was wrapped with ceramic-insulated Ni-chrome wire. Another layer of fiberglass cloth was wrapped around the Ni-chrome wire for insulation. The wire was connected to a variac and used to keep at a constant temperature of about 350°C. Residual MoF_6 from the reactor was reduced on the surface of the heated stainless-steel shavings. The trap was filled with alumina to provide high surface area for absorbing the residual MoF_6 and the SiF_4 produced.

EXPERIMENTAL PROCEDURE

Sample Cleaning

The (100) oriented single crystal silicon wafer was cut into 5cm x 3.5cm size pieces. The slices used for deposition were first soaked in (10:1) fluoric acid solution to remove any oxides and minimize surface heterogeneity. Then it was rinsed with acetone and alcohol to remove organics. All stainless steel flanges and traps were boiled in distilled water and rinsed with acetone and alcohol. Whenever the substrate heater was taken out of the chamber to replace the Ni-chrome wires, it was ultrasonically cleaned and rinsed with acetone and methanol. Gas lines were heated to 100°C to remove water vapor and were always isolated from the air by gas controller valves.

Deposition Procedure

After the liquid nitrogen trap was filled up with liquid nitrogen, the reaction chamber was isolated from the after-burner and alumina trap by closing the exhaust valve, and evacuated to approximately 10^{-7} torr by the diffusion pump. During the evacuation the chamber and the alumina trap wrapped with heating tapes were heated to 180°C to aid in removing adsorbed water vapor. The substrate heater was

also turned on and stabilized at the deposition temperatures of 250 to 400°C during the evacuation. The MoF_6 lines were wrapped with heating tape kept at about 70°C to prevent the MoF_6 from condensing. The after-burner was stabilized at 350°C. The alumina trap and after-burner were pumped down by the roughing pump while heating them to remove water vapor as much as possible..

The reaction chamber and the alumina trap were cooled down. The gate valve was then closed and the exhaust valve was opened. After measuring the chamber pressure before the reaction, i.e. base pressure, helium gas was introduced to temporarily stabilize the exhaust valve at the operating pressures of 1-10 torr by opening the gas control valve. Finally, the MoF_6 gas was introduced into the chamber. A chronograph was immediately turned on and the substrate temperature was manually controlled within $\pm$ 2°C.

At the end of the deposition, the MoF_6 was shut off and the exhaust valve was completely opened. Helium was kept flowing after deposition to purge the system and cool down the substrate. While purging the system with helium, the substrate temperature was reduced. When the substrate temperature fell below 30°C, the chamber was brought to atmospheric pressure with helium and the sample was removed for analysis.

Sheet Resistance Measurement

The sheet resistance, R_S could be directly measured by the 4-point probe method and is expressed in the following equation:

$$R_S = (V/I) \times C.F.$$

where R_S is the sheet resistance of a deposited layer (in Ω/square); V is the measured dc voltage across the voltage probes (in volts); I is the constant dc current passing through the current probes (in amperes); and C.F. is the correction factor that is a function of the sample geometry and the probe spacings. For a large size sample, the correction factor, C.F., approaches 4.53.

Film Thickness Measurement

Two 1cm x 1.5cm samples were prepared for acid etching. Then, the magnitude of each of the samples was measured at two positions of each side with vernier calipus, and averaged for better accuracy. Acid etching was performed with a solution consisting of : 5 ml of H_3PO_4 (85%), 30 ml of HNO_3 (70%), 4 ml of CH_3COOH (99%) and 150 ml H_2O. The 1cm x 1.5cm sample was carefully dipped in the acid solution, agitated gently and weighed. The weight was

measured on a CAHN 29 automatic electrobalance before and after acid etching to calculate the weight of deposited molybdenum film. This balance can measure with an accuracy of 0.1 μg in a balance range of 25 mg to 0.1 μg. However, the balance was operated in a range of 250 mg to 1 μg due to the weight of a piece of silicon to be weighed. In this range, the smallest thickness that can be measured was 10^{-7} cm. The weight measurement was continued until there was no significant change.

The film thickness was calculated from the weight change measured from acid etching by assuming full density of molybdenum (10.2 g/cm^3). The equation is expressed in the following:

$$\text{THICKNESS} = M / (A \times D)$$

where M is the weight change of a silicon sample; A is the area of the sample; and D is the bulk density of molybdenum. The thicknesses of two samples calculated from the above equation were averaged.

AES Analysis

After taking the sample out of the reaction chamber, it was kept in a resealable plastic bag to keep the sample

clean. Later on, the sample was transported to the Center for Research in Surface Science and Submicron Analysis (CRISS) in the Physics Department at Montana State University.

The AES depth profiling analyses were performed by the Physical Electronics (PHI 595) scanning Auger microprobe whose minimum electron beam size is about 50nm. The PHI 595 is completely computer controlled and set up for computer assisted data analysis. One can perform point analysis, line analysis, or two dimensional mapping of any element (except H and He) on the surface of a sample.

A 2mm x 2mm area of a sample was sputtered by a 3kv Argon (Ar^+) ion beam for 0.5 to 2 minute intervals. At the end of each interval, the area sputtered by the ion beam was analyzed by AES. The primary electron beam had a voltage of 3.0 keV and a beam current of approximately 0.2 μA. The composition as a function of depth into the surface could be determined by combining continuous sputter etching with AES. The AES data was recorded digitally on a magnetic disc with the use of a DEC PDP 11/04 computer.

The depth profiles were interpreted semi-quantitatively since the Mo films on the silicon surface deposited by the silicon reduction were not smooth and the impurities were not distributed uniformly through the film,

so that a constant sputter yield could not be obtained at each of the spots sputtered [57]. It is, however, essential for the AES depth equation to be valid. To overcome these problems the AES data were utilized to determine relative amounts of molybdenum and impurities present.

SEM Analysis

The SEM analyses were also carried out at the CRISS lab. A scanning Electron Microscope equipped with the Auger unit offers both secondary electron and absorbed current imaging, and it provides electron micrographs at magnifications up to 100,000X. However, 1000X magnification was used for all samples investigated in order to obtain the best resolution.

RESULTS AND DISCUSSION

The results of experiments at the pressures of 10 torr and 1 torr while varying the deposition temperature from 250 to 400°C and the deposition time from 5 to 60 min. are shown in Figures 2 through 5. These results were obtained at the constant flow rates of 3 sccm and 9 sccm of MoF_6 and He gases, respectively.

Effect of Deposition Parameters on Film Thickness

In Figure 2 and Figure 3 the film thickness generally increases for a limited time, afterwhich no further growth occurs. For example, the films deposited at 250°C self-limit on the average at about 115 nm of assumed full-density Mo film. It is generally known that CVD Mo and W films, deposited at a variety of temperatures, are all less than full density and rough. In particular, the percentage of space occupied by trapped gas and pores in the CVD W was reported to be up to 58.8 % [6]. Hence, acid dissolution will be more effective than SEM cross-sectioning in determining the thickness of the film deposited by chemical vapor deposition. In the temperature range of 300 to 350°C film thickness self-limits at about 120 nm. Thickness vs.

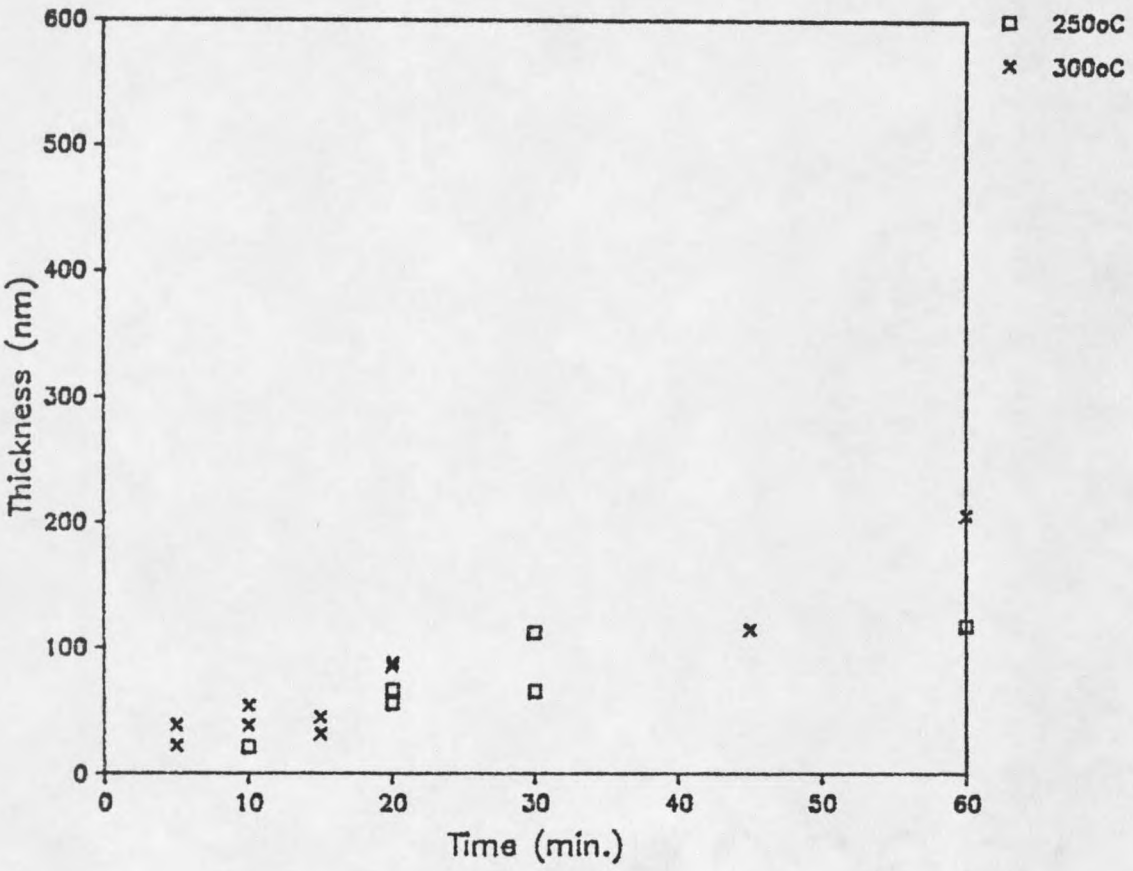

Figure 2. Thickness of Deposited Mo Film on (100) Si as a Function of Deposition Time at T = 250°C, 300°C and P_{tot} = 10 torr

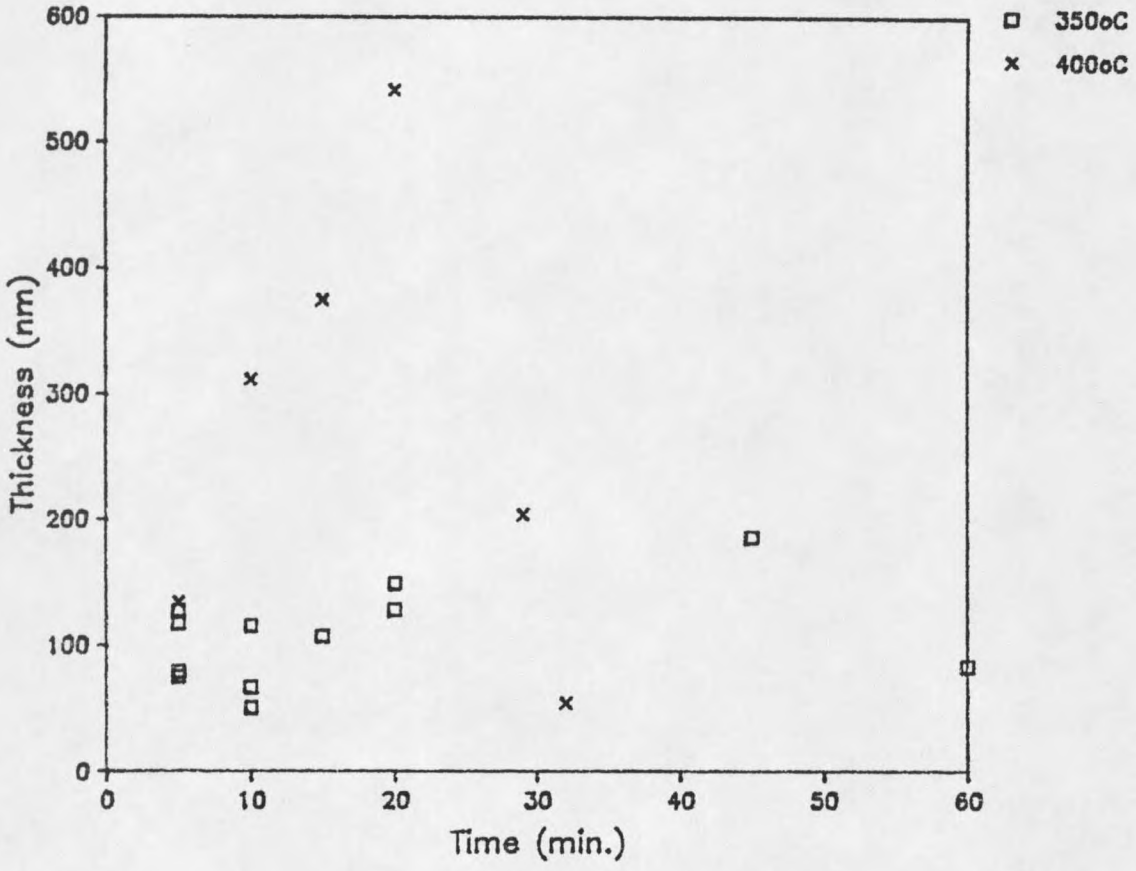

Figure 3. Thickness of Deposited Mo Film on (100) Si as a Function of Deposition Time at T = 350°C, 400°C and P_{tot} = 10 torr

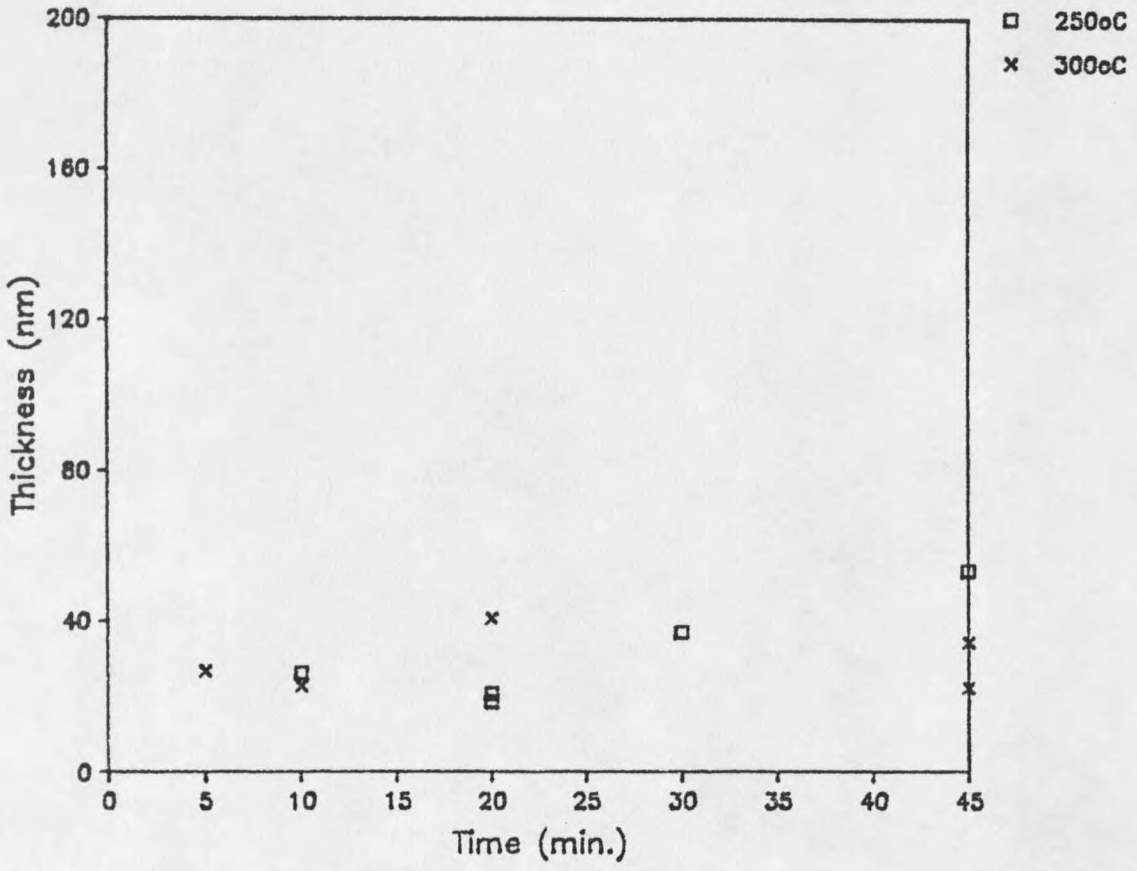

Figure 4. Thickness of Deposited Mo Film on (100) Si as a Function of Deposition Time at T = 250°C, 300°C and P_{tot} = 1 torr

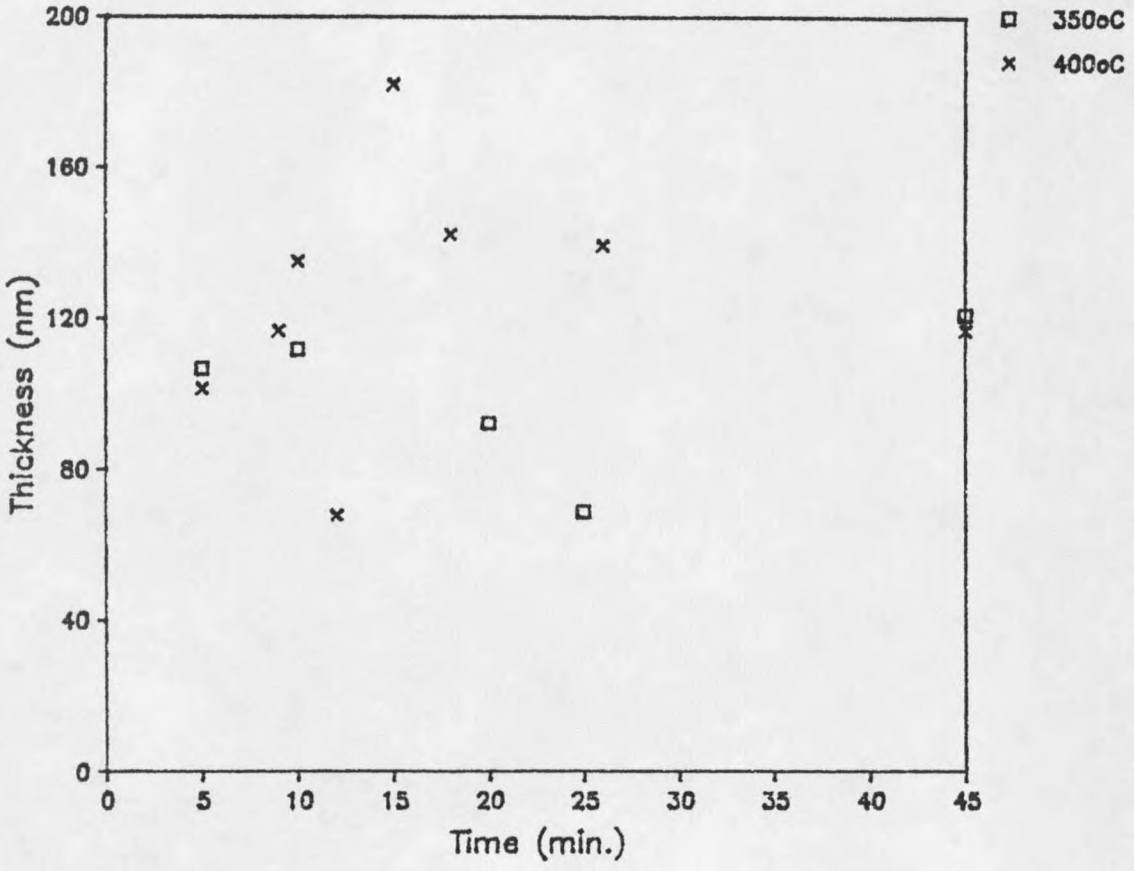

Figure 5. Thickness of Deposited Mo Film on (100) Si as a Function of Deposition Time at T = 350°C, 400°C and P_{tot} = 1 torr

time at 300°C, however, shows ambiguous self-limiting behavior since it can be correlated with a linear relation. More data is required between 20 min. and 45 min. to clearly state if the relation is self-limiting or not at 300°C. The film growth at 400°C stops after reaching up to 540 nm. The self-limiting thicknesses are approximated for various operating conditions and given in Table 2. There appears to be no temperature dependence of self-limiting thickness for the films deposited at 250-350°C. In addition, the self-limiting thickness at 400°C is difficult to determine due to a rapid increase of film thickness.

Table 2. The Approximated Self-Limiting Mo Thicknesses at Operating Conditions

Pressure torr	Temperature °C	Self-Limiting Thickness nm
10	250	115
10	300	120*
10	350	115
10	400	540**
1	250	32
1	300	31
1	350	113
1	400	182

*This value was calculated from unclear self-limiting relationship.
**This value was the maximum thickness at the operating condition.

Figure 4 and Figure 5 also show self-limiting of film deposition at 1 torr, but the self-limiting thickness is less at the same temperature and the higher pressure. For example, the films deposited at 300°C and 1 torr self-limit at about 31 nm, compared to about 120 nm at 300°C and 10 torr (see also Table 2). There is apparently no significant change in thickness at 350°C for the two pressures.

From Figures 2 through 5, it is clear that the silicon reduction reaction of MoF_6 does in fact result in self-limiting films, but not all films are self-limiting at the same thickness, and the deposition rate of molybdenum film on silicon is not constant with respect to time. Once a Mo film is deposited over the entire silicon surface by the silicon reduction, the deposition rate decreases to zero, meaning that no further growth occurs after a limiting thickness has formed.

The temperature and total pressure dependence of the self-limiting nature has been reported in the case of silicon-reduced W films by several researchers [8,22,30,32,34]. However, McConica and Krishnamani [31] reported somewhat different results. The thickness of the deposited tungsten was found to be self-limiting over a time range of 1 to 20 minutes and temperature range of 250

to 375°C. In this study, gradual growth of the films deposited at 10 torr, however, is observed up to 30 minutes of deposition time. An abrupt increase and decrease of the film thickness is observed at 400°C and 10 torr (see Figure 3). Broadbent [34] observed a similar pattern at the pressure of 0.5 torr and the temperatures of 300 and 475°C for tungsten deposition. According to his results, thickness of tungsten films on silicon was increased or decreased abruptly or gradually as deposition proceeded for long periods. Even though the film thickness at high temperature was not assured to be greater than at low temperature, high temperature deposition produced thicker film in most cases.

It is generally believed that W and Mo films are formed by the same mechanism, that of fluoride percolation through the porous metal film. However, there is significant difference on the self-limiting nature of the silicon-reduced Mo, even if this study agrees well with the literature findings on the silicon-reduced W film. Woodruff and Sanchez-Martinez [12], whose study for the silicon reduction of MoF_6 was carried out in a hot-wall, low-pressure CVD reactor in N_2 ambient gas, reported that the reaction of MoF_6 with silicon proceeded with no self-limiting behavior in a temperature range of 20 to 500°C and

at pressures between 2 and 5 torr. They observed 9.2 microns of molybdenum film. Lifshitz et al. [35] also observed that the silicon reduction reaction of MoF_6 was not self-limiting in a hot wall reactor, in contrast to the analogous reaction between WF_6 and silicon. Especially, they observed a linear growth of the films as thick as several microns with respect to deposition time. Such thick films were never observed in this study. However, even though the silicon displacement reaction in the CVD W deposition has been conventionally believed to result in thin (~10nm) self-limiting films of W, very thick films were also observed by Tsao and Busta (~200nm) [10], and Mianowski et al. (~600nm) in N_2 ambient at atmospheric pressure [33]. Therefore, we may not exclude the possibility of observing very thick films as well as thin films from the silicon reduction of MoF_6. Moreover, linear growth of a molybdenum film was observed for a limited time (i.e. 20 min. at 400°C and 10 torr). It may be due to the differences in various factors such as sample cleaning method [3,33], silicon doping level [3], and CVD reactor type. In particular, Broadbent and Stacy [37] reported very interesting results generated on samples that were introduced into a cold furnace and then heated under vacuum. Their deposition procedure was very similar with that used in this study.

The only difference is that the present reaction chamber was not cooled with water as in the case of a typical cold-wall reactor. Their results showed almost no temperature dependence of W film thicknesses in a temperature range of 300 to 500°C. In addition, their film thicknesses were extremely smaller than those of Green et al.'s [6] which were grown in a hot wall reactor. This may be due to some effects of reactor type on reaction mechanisms. This effect can be understood by surface chemistry studies.

A sharp decrease of the film thickness vs. time obtained at the temperature of 400°C and at the pressures of 1 and 10 torr shown in Figure 3 and Figure 5 suggests a severe etching of the films by MoF_6. Shroff and Delval [14] reported in the study of CVD W and Mo that at low temperatures and low pressures there took place chemical etching of the substrate by the reaction products and the unreacted gases. However, in our study the etching effect was not so severe at low temperatures. The most severe etching was observed at a temperature of 400°C and at a pressure of 10 torr. This may indicate that the etching of the deposited Mo film mainly resulted from MoF_6, which is supported by relatively low etching rate at 400°C and 1 torr. The etching effect was also observed by Pauleau and Lami [2] and Tsao and Busta [10] in the case of CVD W films.

Film Surface Morphology

SEM micrographs of the film surface have been taken for samples deposited at 250°C and 400°C at 10 torr. Figure 6(a) and Figure 6(b) depicts a film deposited at 250°C and 10 torr, which is approximately 112 nm thick. These pictures were taken at the middle of the sample before and after sputtering the surface for 16 min. The film before sputtering, shown in Figure 6(a), has a rough surface, and after sputtering not much change in roughness is observed except revealing small voids (Figure 6(b)) which were not visible before sputtering. The voids were always present in the films investigated by SEM.

The SEM micrographs in Figure 7 were taken before sputtering at two different locations of a sample whose thickness (117.5 nm) is almost the same as that of the film shown in Figure 6, in order to observe the roughness of the film at different spots on the sample surface. The area shown in Figure 7 (a) seems rougher than the one in Figure 7 (b). Such a non-uniformity of the deposit may be caused by localized thermal gradients and localized depletion of MoF_6 in the feed gas [41]. The surface roughness of the films may also occur as a result of the randomness of the deposition process and (or) of the presence of contamination on the substrate (or in the vapor phase) during deposition

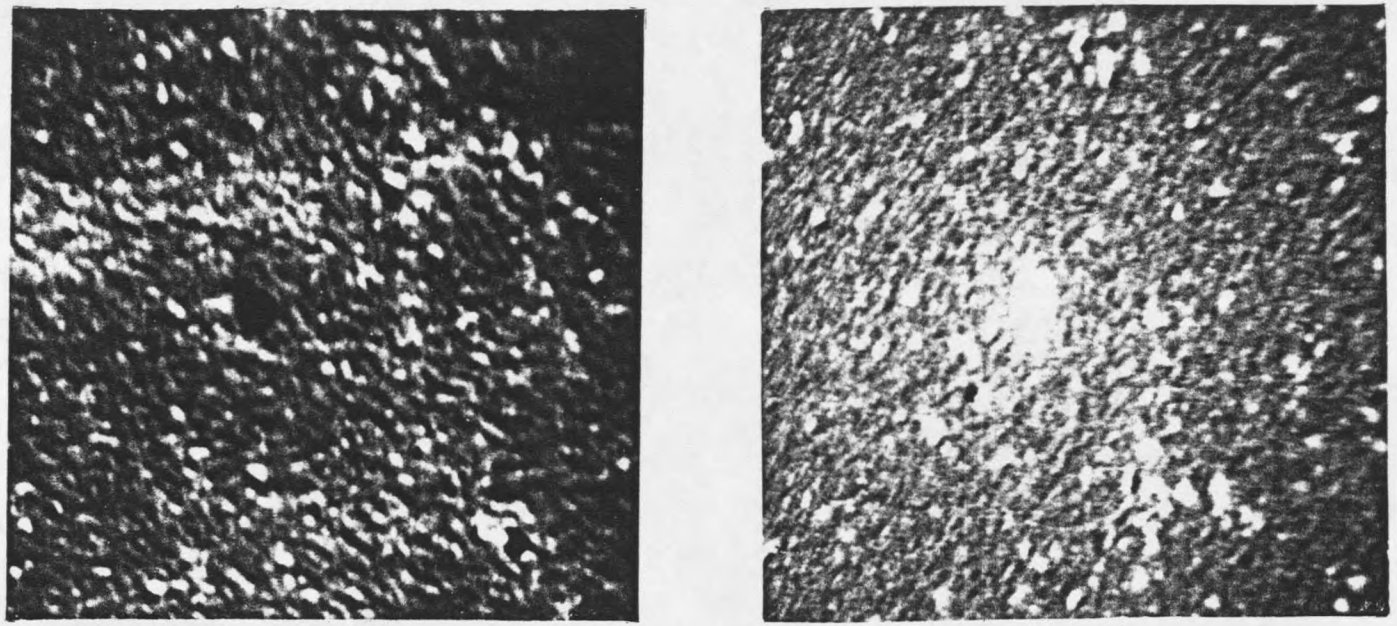

(a) 1,000 X (b) 1,000 X

Figure 6. SEM Surface Micrographs of a Mo Film Deposited at T = 250°C and P_{tot} = 10 torr (30min.)

(a) before sputtering (b) after sputtering

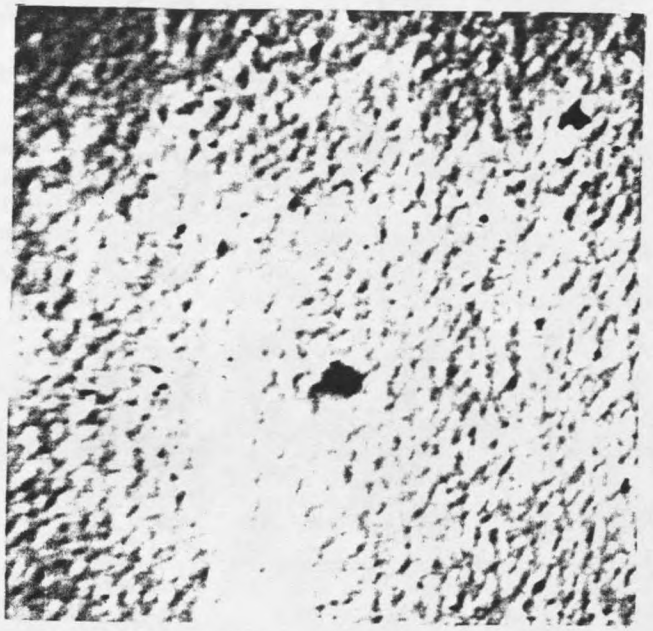

(a) 1,000 X

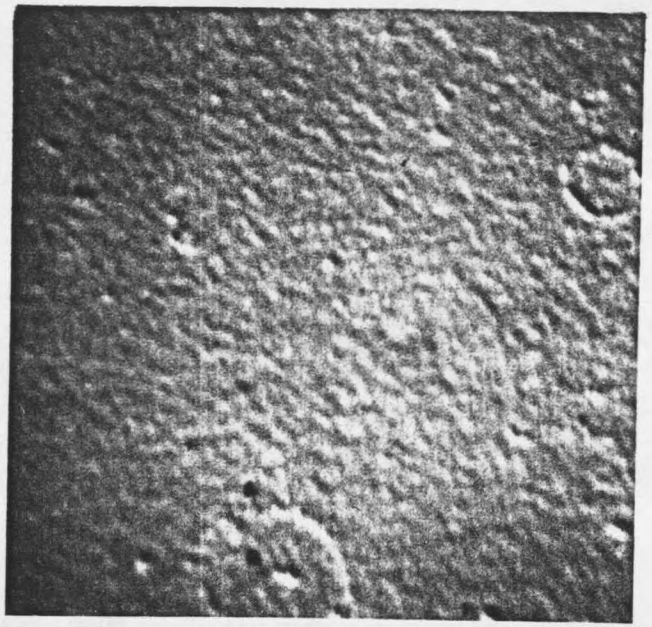

(b) 1,000 X

Figure 7. SEM Surface Micrographs of a Mo Film Deposited at T = 250°C and P_{tot} = 10 torr (60min.)

(a) location 1

(b) location 2

[58]. Another possible reason for surface roughness is localized etching.

Figure 8 shows a film deposited at 400°C and 10 torr, whose thickness is 3 times those of Figure 6 and Figure 7. With increasing temperature from 250 to 400°C, the appearance of the deposit changes from rough to smooth. It is known that depositions at high temperatures tend to show less surface roughness. This is because increased surface mobility from the higher substrate temperatures can lead to filling of the peaks and voids. On the other hand, higher temperatures can also lead to the development of crystal facets, which may continue to grow in favored directions, leading to increased surface roughness. Ohba et al. [59] reported that in the case of H_2 reduction of WF_6 the surface of the low temperature deposition was smoother than the surface of the high temperature deposition. In a study of CVD of W and Mo by Shroff and Delval [14], SEM micrographs of the surface and the cross-section of the deposits revealed very small voids or bubbles whose number tends to increase with increasing H_2/MoF_6 ratio and pressure, and decrease with increasing deposition temperature.

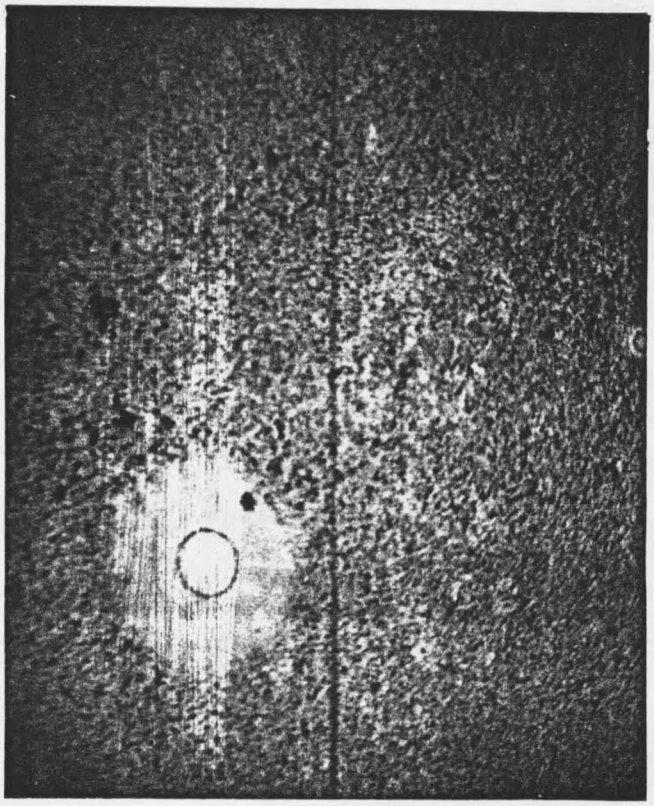

1,000 X

Figure 8. SEM Surface Micrograph of a Mo Film Deposited at T = 400°C and P_{tot} = 10 torr (15min.)

Sheet Resistance

Figure 9 and Figure 10 show the sheet resistance measured by the 4-point probe method. The self-limiting nature can also be understood from these figures. The sheet resistance of the films deposited at 250°C in Fig 9 becomes constant and does not change appreciably for thicker films. It is also noted that the sheet resistance of Mo films deposited at 300°C decreases from a high value for thin films to a low value for thick films. Even though there is some scattering of data, the general trend is obvious. Also, there is much greater scattering in sheet resistance at 350°C as seen in Figure 10, but the general trend is the same. At 400°C the sheet resistance becomes constant when the film thicknesses are greater than 100 nm.

Mianowski et al. [33] reported that an unusual dependence of the sheet resistance would be due to the large numbers of pores forming inside of the films during the deposition. The influence of the pores on the sheet resistance could not be understood from this study due to the absence of data on the porosity. That very thick films above 300 nm show low sheet resistance may account for how critically the porosity affects the change of the sheet resistance. As reported in a study by Lifshitz and Green [36], thick films may contain less porosity due to filling

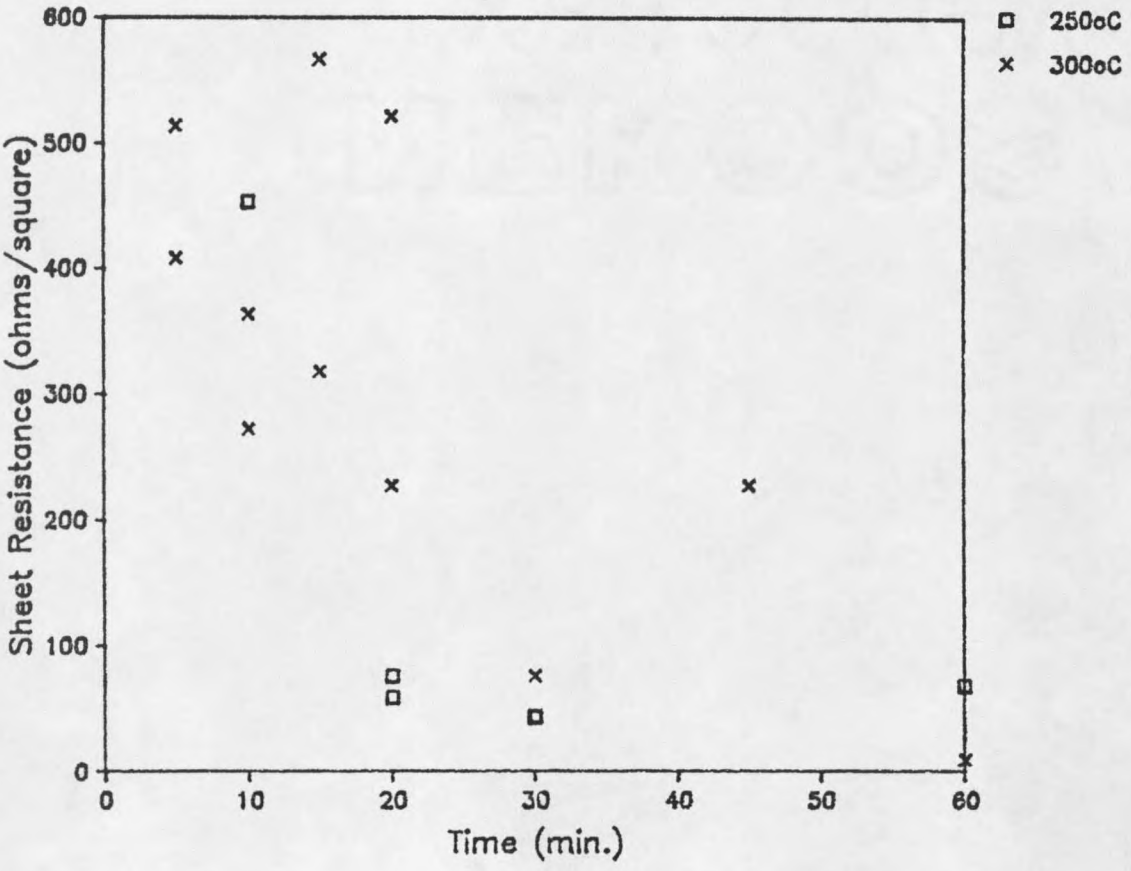

Figure 9. Sheet Resistance versus Deposition Time at T = 250°C, 300°C and P_{tot} = 10 torr

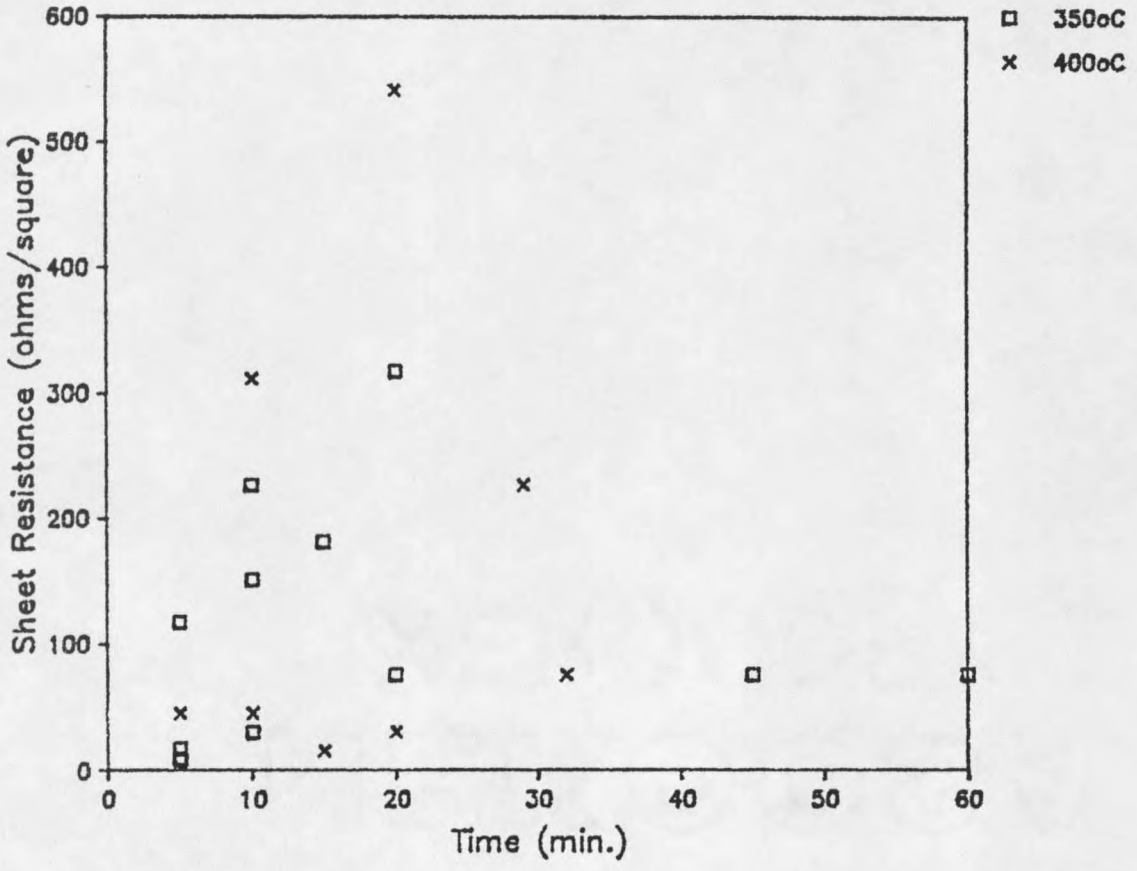

Figure 10. Sheet Resistance versus Deposition Time at T = 350°C, 400°C and P_{tot} = 10 torr

of small pores as well as large fissures by continuously growing molybdenum particulates. The other factor for increasing the sheet resistance is the non-uniformity of films, which was also observed while measuring the sheet resistance at different locations on the film.

Impurity Content

Impurities captured in LPCVD Mo films were analyzed by AES. Fluorine, oxygen, and carbon were the impurities which were examined. Some other metals such as Al, Ni (or Co), Cr (or Fe) were also detected from the SIMS analysis. However, these impurities were neglected due to the source from which they originated. For example, Al came from the Al foil because the plastic container for fluoric acid was covered with the foil, which was dissolved later by corrosion. All of these metal impurities were detected from the bare silicon wafer just after cleaning it with the acid. The other metals except Al might come from the stainless steel analysis vacuum chamber of the instrument or the reaction chamber where the deposition was carried out. In this study, severe corrosion of flexible stainless steel tube occurred when MoF_6 gas was condensed in the gas line. Therefore, MoF_6 gas may also erode the inside of reaction chamber during the deposition. Another possible source of

these metals may be the corrosion of Ni-chrome wires used to heat the substrate holder, which caused, later on, the break-down of the wires.

Figure 11 shows an AES depth profile of a sample deposited at 10 torr of total pressure and temperature of 400°C. It shows high F content, relatively low oxygen and carbon content. In Figure 11 the oxygen content is lower, compared with that in Figure 12. Many studies reported that the W and Mo films deposited over silicon via silicon or hydrogen reduction were high in oxygen content and extremely porous [12,31,35,36,47]. Such porosity allows oxygen to move freely through the highly developed pores in the film and form a surface metal oxide. It was also reported that the oxygen content depended on the temperature at which the reactor was opened to air [36]. In this study all of the samples were exposed to air below 30°C. However, the oxygen content was extremely high at all conditions but at 400°C and 10 torr. Also, the oxygen content was not significantly influenced by base pressure, which is a pressure of the reaction chamber just before starting the reaction. Table 3 is included to better understand the change of the impurity content with respect to operating conditions.

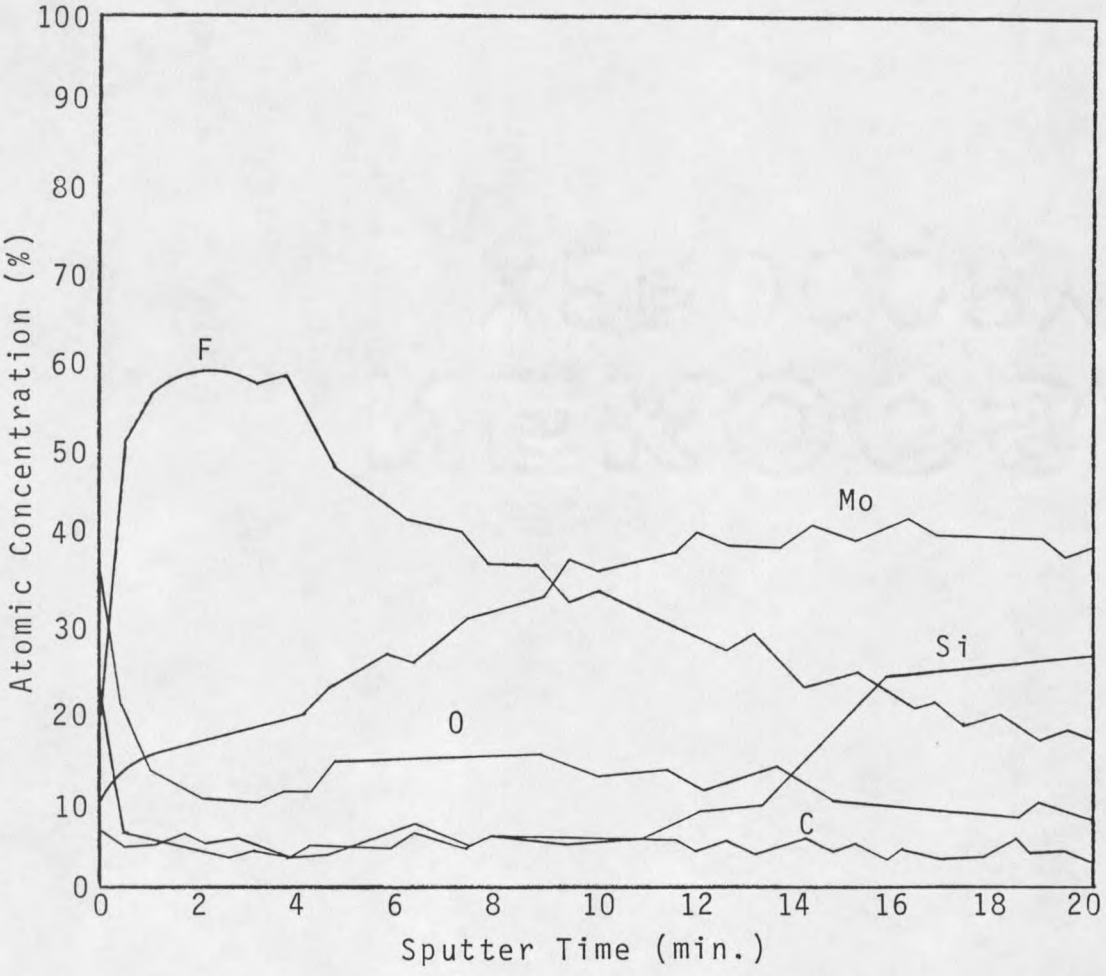

Figure 11. AES Depth Profile of a Mo Film Deposited at $T = 400^{o}C$ and $P_{tot} = 10$ torr (10min.)

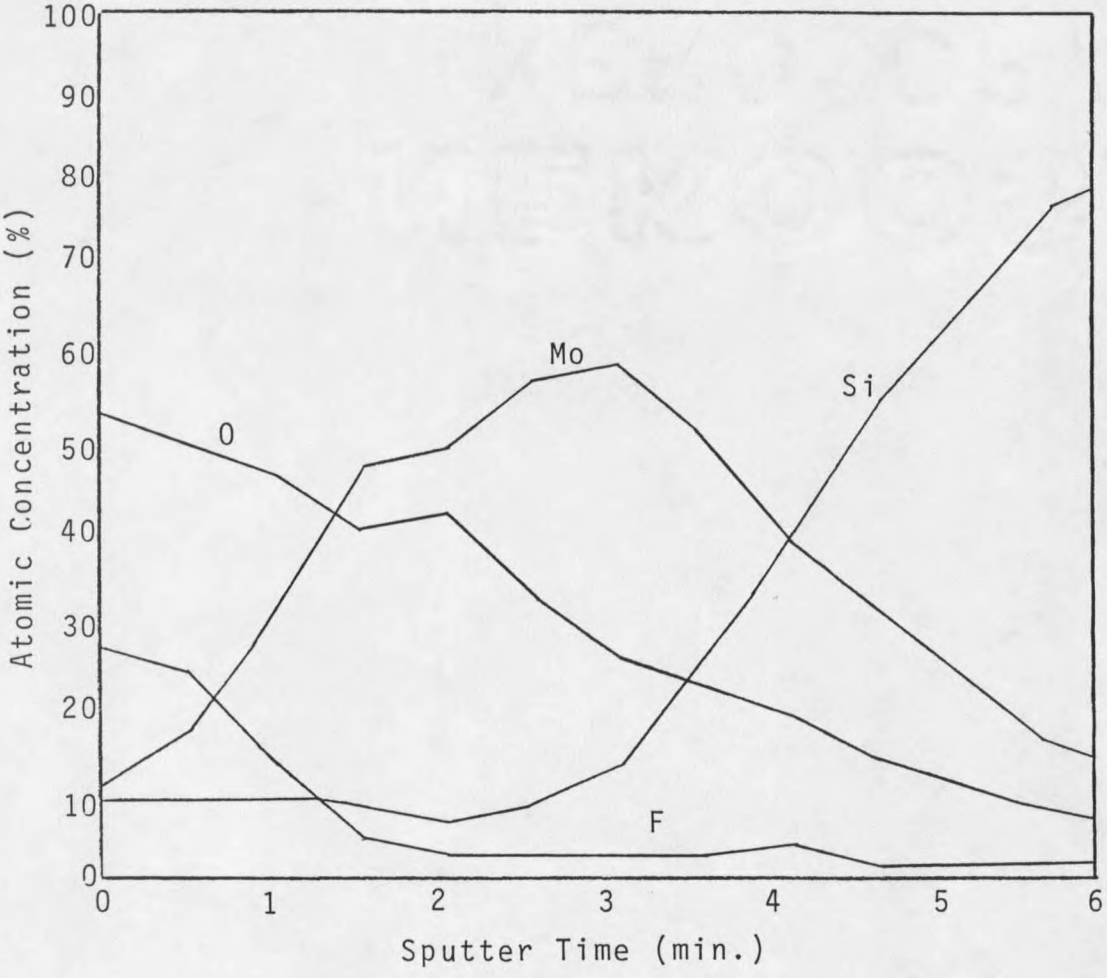

Figure 12. AES Depth Profile of a Mo Film Deposited at $T = 400^{\circ}C$ and $P_{tot} = 1$ torr (10min.)

Table 3. Relative Amounts of Film Impurities from AES Depth Profiles at Highest Mo Peak Value.

Press. torr	Temp. °C	Time min.	Base press. torr	Thick. nm	Relative amount of impurities %				
					Mo	Si	O	F	C
10	250	30	0.004	65.0	48	19	26	0	7
10	250	60	0.004	56.0	49	12	29	0	10
10	300	5	0.003	38.0	32	14	31	5	18
10	300	10	0.005	38.0	35	13	29	5	18
10	300	60	0.006	206.0	65	11	16	6	2
10	350	5	0.003	75.0	53	17	26	4	0
10	350	10	0.005	115.0	60	9	26	5	0
10	400	10	0.002	311.0	42	25	8	21	4
10	400	15	0.004	374.0	55	11	7	22	5
10	400	20	0.005	540.0	64	15	9	12	0
1	300	20	0.009	40.0	48	29	17	6	0
1	350	5	0.002	107.0	40	26	16	11	7
1	400	5	0.015	101.0	45	23	29	3	0
1	400	10	0.015	135.0	57	15	25	3	0
1	400	18	0.048	142.0	50	12	27	6	5

In Figure 11 the oxygen is well distributed at much reduced content through the film. In particular, the amount of total oxygen captured in the film decreased as deposition time changed from 10 to 20 min. During the change the film thickness increased from 310 to 540 nm. Figure 12 was obtained from a sample having 135 nm thickness. Considering that the oxygen can diffuse through the pores in the film, it is speculated from the above fact that thick films above 300 nm may contain very fine

continuous pores with less porosity. This speculation is supported by the oxygen depth profile shown in Figure 13, which was obtained from a sample having 206 nm in thickness. Other samples having the same amount of oxygen at the highest Mo peak showed that the oxygen content was much greater through the film. However, details could not be understood due to the absence of the data on the porosity and the pore size distribution.

The fluorine content, however, changes somewhat differently, as shown in Table 3. In Figure 11 a large amount of fluorine is observed at the outermost layer of the film, which gradually decreased as the sputtering continued The fluorine content in Figure 12 is only high at the outermost layer of the film. High content of fluorine in the films was observed at 400°C and 10 torr, the extent of which decreased as the deposition temperature varied from 400 to 250°C. It has been reported that MoF_6 gas decomposes into subfluorides (i.e., MoF_5, MoF_4) upon the adsorption onto the silicon surface and the subfluorides may react with the bare Si surface, forming reaction products such as SiF_4, SiF_3, SiF_2, and SiF. Carlsson and Boman [60] reported on the reaction product generated from the silicon reduction reaction of WF_6. Their study was carried out to

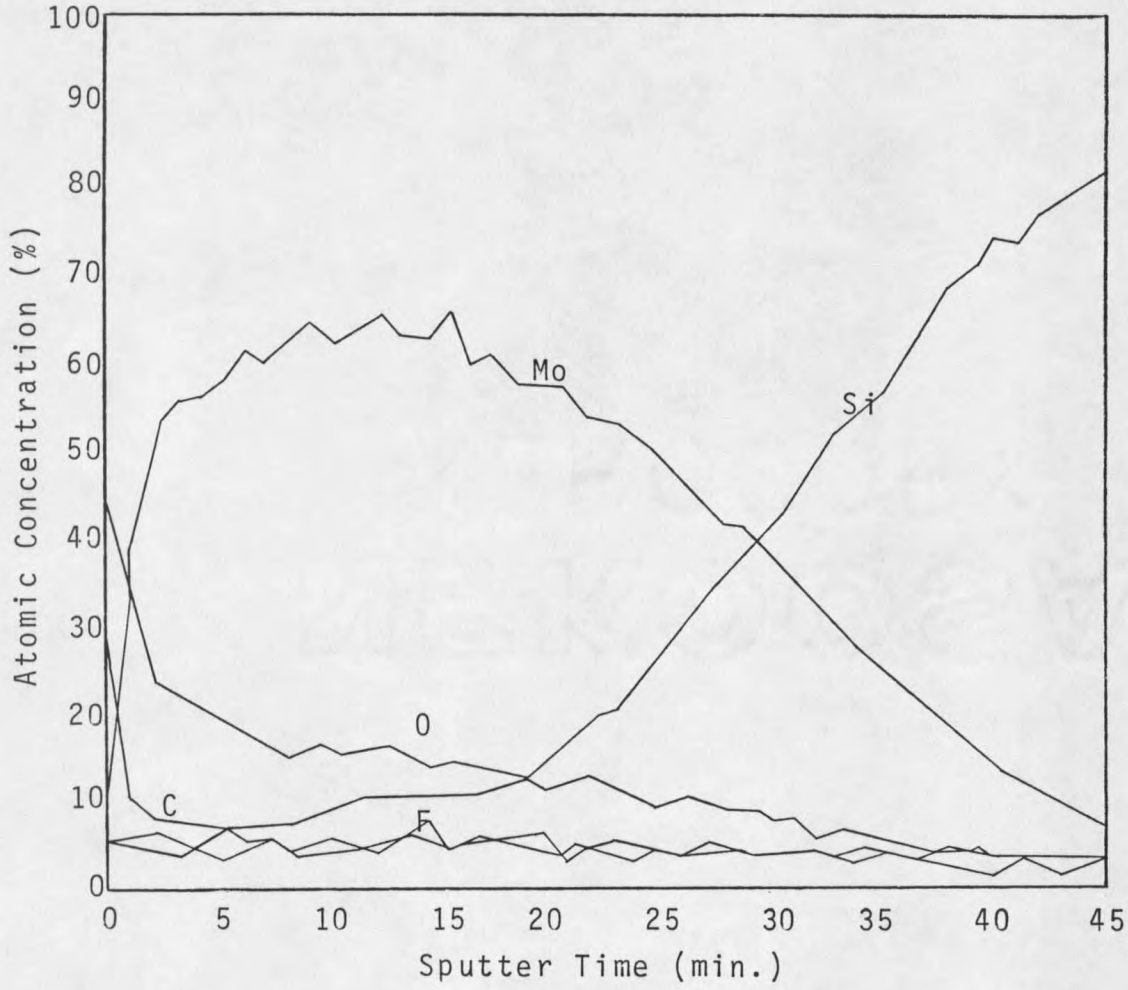

Figure 13. AES Depth Profile of a Mo Film Deposited at T = 300°C and P_{tot} = 10 torr (min.)

predict the change of reaction products in terms of temperature, in which the main reaction product, SiF_4 was preferred at low temperatures and large amounts of lower fluorides were expected at high temperatures. Creighton [61] also examined the reaction occurring on a WF_x-covered SiO_2 surface by a temperature programmed desorption (TPD) method. The resulting TPD spectrum showed that tungsten subfluorides desorbed from tungsten surfaces exposed to WF_6 at significant rates at normal CVD temperatures (250-400°C). Especially, the major desorbing ion in the TPD spectrum was the WF_4^+, indicating that the parent molecule should be the WF_5. This is supported by the WF_6 mass spectrum [62] in which the WF_5^+ signal is most intense.

It seems obvious that the MoF_6 decomposes into the subfluorides upon adsorbing on the silicon surface, and the extent of the decomposition depends on the substrate temperature. Also the etching effect seems influenced by decomposition of MoF_6 molecules into subfluorides since the decomposition rate upon adsorption will probably be higher at high temperatures (350°C, 400°C), producing large amount of fluorine. This fluorine may react with deposited Mo to form molybdenum subfluorides which are considered to be volatile [36].

High fluorine content is observed at the surfaces of the films deposited at 400°C (see Figures 11 and 12). As temperature varies from 400 to 250°C, the total fluorine content (peak area of depth profile) decreases and finally becomes zero. Such a high fluorine content at the surface may be due to unreacted subfluorides adsorbed on the substrate by chemical bonds, the amount of which is presumably greater at high temperatures. Since the temperature of the substrate was decreased rapidly after shut-down of the power, the adsorbed molecules would remain unreacted on the surface upon cooling. Much of decomposed fluorine will easily diffuse through the pores into the film on account of their smaller size. Shroff [47] reported that all the samples had lower fluorine content for high ratios of H_2/WF_6. This may be easily understood because the decomposed fluorine will react with excessive hydrogen to form HF gas before diffusing into the pores. Therefore, the total amount of fluorine being diffused through the pores in the film will be significantly reduced.

SUMMARY AND CONCLUSIONS

The objective of this study was to investigate the deposition kinetics of the silicon reduction reaction of MoF_6 gas and the film morphology, and compare with the findings reported on LPCVD W and Mo films. The important findings of this study are as follows:

1. LPCVD Mo film deposited by the silicon reduction reaction did self-limit at the operating conditions carried out in this study, as do the silicon-reduced W films. The silicon-reduced Mo films self-limited at different thickness depending on the temperature and the total pressure.

2. The etching effect by MoF_6 was most severe at 400°C and 10 torr, and was also observed at all other conditions to a lesser extent.

3. Analyses of the AES depth profiles of the CVD Mo films showed that oxygen content was as high as 31%, and thin films always contained a larger amount of oxygen than the thick films. Thick films (above 300 nm) incorporated less oxygen. The impurity was as low as 8%. Since there was an extremely low amount of oxygen in the

reaction chamber during the reaction on account of low base pressure, the oxygen was thought to be captured in the sample after removing it from the reaction chamber.

4. Fluorine content was extremely high at the surfaces of the films, especially when deposition was carried out at 400°C and 10 torr. Low F content at 400°C and 1 torr suggested that decomposition of molybdenum hexafluoride into lower fluorides and fluorines upon adsorption was limited by low sticking probability under low pressures.

5. The sheet resistance was high because the films were probably porous and rough and incorporated large amounts of oxygen and fluorine.

RECOMMENDATIONS

Based on the results of this experiment and the literature review, the following recommendations are made:

1. A transmission electron microscopy (TEM) study is needed to observe the change of pores and voids in the growth of the films.

2. More surface chemistry work seems necessary to understand the etching of the deposited film by molybdenum hexafluoride because the etching effect was not severe at low temperatures, which means the erosion of the film by MoF_6 is not as simple as we think.

3. The difference between hot-wall and cold-wall reactors needs to be understood as to deposition kinetics and film morphology.

REFERENCES CITED

REFERENCES CITED

1. Brown, D.M. J. Electrochem. Soc., 114, 730, (1967).

2. Pauleau, Y., and Lami, Ph. J. Electrochem. Soc., Vol. 132, No. 11, 2779-2784, (1985).

3. Bryant, W.A., and Meier, G.H. J. Electrochem. Soc., Vol. 120, No. 4, 559-565, (1973).

4. Bryant, W.A. J. Electrochem. Soc., Vol. 125, No. 9, 1534 -1543, (1978).

5. Broadbent, E.K., and Ramiller, C.L. J. Electrochem. Soc., Vol. 131, No. 6, 1427-1433, (1984).

6. Green, M.L.; Ali, Y.S.; Boone, T.; Davidson, B.A.; Feldman, L.C.; Nakahara, S. in "Tungsten and Other Refractory Metals for VLSI Application II", E.K. Broadbent, Ed., MRS, Pittsburg, 1986.

7. Cheung, H. Nucl. Sci. Abstr., 26(12), 28599, (1972).

8. Tracy, M.E. in "Tungsten and Other Refractory Metals for VLSI Applications", R.S. Blewer, Ed., MRS, Pittsburg, 1985.

9. Paine, D.C.; Bravman, J.C.; Saraswat, K.C. in "Tungsten and Other Refractory Metals for VLSI Applications", R.S. Blewer, Ed., MRS, Pittsburg, 1985.

10. Tsao, K.Y., and Busta, H.H. J. Electrochem. Soc., Vol. 131, No. 11, 2702-2708, (1984).

11. Sahin, T.; Flanigan, E.J.; Sears, J.T. in "Tungsten and Other Refractory Metals for VLSI Applications II", E.K. Broadbent, Ed., MRS, Pittsburg, 1986.

12. Woodruff, D.W., and Sanchez-Martinez, R.A. in "Tungsten and Other Refractory Metals for VLSI Applications II", E.K. Broadbent, Ed., MRS, Pittsburg, 1986.

13. Stull, D.R., and Prophet, H. JANAF Thermochemical Tables, 2nd edition, National Bureau of Standards, Washington, DC, 1971.

14. Shroff, A.M., and Delval, G. High Temperatures-High

Pressures, Vol. 3, 695, (1971).

15. Murarka, S.P. in "VLSI Technology", S.M. Sze, Ed., 2nd edition, p. 377, McGraw-Hill, New York, 1988.

16. Blewer, R.S., and Wells, V.A. Proc. 1st IEEE VLSI Multilevel Interconnection Conf., New Orleans, June 1984, IEEE Cat. #84CH1999-2, p. 153.

17. Green, M.L., and Levy, R.A. J. Electrochem. Soc., 132, 1243, (1985).

18. Wilson, R.H. "The Use of Selective Tungsten Deposition. Achieving the Goals of the 1/4 μm CMOS Technology", SRC Topical Research Conference, 1/4 μm CMOS Technology, Cornell University, Ithaca, N.Y., Dec., 1985.

19. Kern, W., and Ban, V. in "Thin Film Processes", J.L. Vosseu and W. Kern, Eds., p. 257-331, Academic Press, New York, 1978.

20. Hammond, M. Solid State Technol., Dec., 61, (1979).

21. Kern, W., and Schnable, G.L. IEEE Trans., ED-26, 647, (1979).

22. Singer, P. "Techniques of Low Pressure CVD", Semiconductor Intl., p. 72, May, 1984.

23. Rosler, R.S. Solid State Technol., 20(4), 63, (1977).

24. Wolf, S., and Tauber, R.N. "Silicon Processing for the VLSI Era: Process Technology", Lattice Press, California, p. 169, 1986.

25. Gargini, P.A., and Beinglass, I. IEDM Tech. Dig., CH1708 -7/81, 54, (1981).

26. Miller, M.E., and Beinglass, I. Solid State Technol., 25, 85, (1982).

27. Saraswat, K.C.; Swirhun, S.; McVittie, J.P. in "VLSI Science and Technology 1984" K.E. Bean, and G.A. Rozgonyi, Eds., p. 409, The Electrochemical Society Softbound Proceedings Series, Pennington, NJ, 1984.

28. Moriya, T.; Shima, S.; Hazuki, Y.; Chiba, M.; Kashiwagi, M. IEDM Tech. Dig., CH1973-7/83, 550, (1983).

29. Nicolet, M-A. in "Tungsten and Other Refractroy Metals for VLSI Era II", E.K. Broadbent, Ed., MRS, Pittsburg, 1986.

30. Beinglass, I. in "Tungsten and Other Refractory Metals for VLSI Applications", R.S. Blewer, Ed., MRS, Pittsburg, p. 16, 1985.

31. McConica, C.M., and Krishnamani, K. "The Kineticss of LPCVD Tungsten Deposition in a Single Reactor", AICHE Seattle Meeting, 1985.

32. Moriya, T., and Itoh, H. in "Tungsten and Other Refractory Metals for VLSI Applications", R.S. Blewer, Ed., MRS, Pittsburg, p. 22, 1985.

33. Mianowski, R.J.; Tsao, K.Y.; Waggener, H.A. in "Tungsten and Other Refractory Metals for VLSI Applications", R.S. Blewer, Ed., MRS, Pittsburg, p. 146, 1985.

34. Broadbent, E.K. in "Tungsten and Other Refractory Metals for VLSI Applications", Editor, MRS, Pittsburg, p. 369 1984.

35. Lifshitz, N., and Brown J.M. in "Tungsten and Other Refractory for VLSI Applications II", E.K. Broadbent, Ed., MRS, Pittsburg, p. 23, 1986.

36. Lifshitz, N., Green, M.L. J. Electrochem. Soc., Vol. 135, No. 7, 1833, (1988).

37. Broadbent, E.K., and Stacy, W.T. Solid State Tech., 51, (1985).
38. Green, N., and Levy, R.A. ibid., 132, 1243, (1985).

39. Lifshitz, N.; Brown, I.M.; Capio, C.O.; Williams, D.S. J. Electrochem. Soc., 134, 2061, (1987).
40. Jaeger, R.R., and Cohen, S.T. Third International Conference on Chemical Vapor Deposition, 500, (1972).

41. Sugano, T.; Chou, H.; Yoshida, M.; Nishi, T. Japanese J. of Applied Physics, 7(9), 1028, (1968).

42. Seto, D.K.; Doo, V.Y.; Dash, S. Second International Conference on Chemical Vapor Deposition, 659, (1970).

43. Hieber, K., and Stoltz, M. Fifth International Conference on Chemical Vapor Deposition, 437, (1975).

44. Kaplan, L.H., and d'Heurle, F.M. J. Electrochem. Soc., 117(5), 693, (1970).

45. Carver, G.E., and Seraphin, B.O. Appl. Phys. Lett., 34 (4), (1979).

46. Flanigan, E.J. Master's Thesis, Montana State University, Bozeman, Montana, July, 1987.

47. Shroff, A.M., Thomson-CSF "Influence of the Pressure on the Deposition Characteristics of CVD Tungsten", 6th Plansee Seminar 1968, edited by Benesovsky, Springer Verlag, 1969.

48. Chen, L.J.; Hung, L.S.; Mayer, J.W. Applications of Surface Science, 11/12, 202-208, (1982).

49. Van Der Putte, P. in "Tungsten and Ohter Refractory Metals for VLSI Applications II", E.K. Broadbent, Ed., MRS, Pittsburg, p. 78, 1986.

50. Pauleau, Y.; Lami, Ph.; Minghetti, B.; Tissier, A. in "Tungsten and Other Refractory Metals for VLSI Application", R.S. Blewer, Ed., MRS, Pittsburg, p. 137, 1985.

51. MacLaury, M.R.; Stoll, R.W.; Woodruff, D.W. in "Tungsten and Other Refractory Metals for VLSI Applications", R.S. Blewer, Ed., MRS, Pittsburg, p. 467-473, 1985.

52. Stacy, W.T.; Broadbent, E.K.; Norcott, M.H. J. Electrochem. Soc., 131, 444, (1985).

53. Goldstein, J.I "Scanning Electron Microscopy and X-Ray Microanalysis, Plenum, New York, 1981.

54. Wolf, S., and Tauber, R.N. "Silicon Processing for the VLSI Era: Process Technology", Lattice Press, California, p. 593, 1986.

55. Sze, S.M. "VLSI Technology", McGraw-Hill, New York, 1st edition, p. 512, 1983.

56. Palmberg, D.W. in "Electron Spectroscopy" D.A. Shirley, Ed., p. 835-859, North-Holland, Amsterdam, 1972.

57. Sahin, T. Personal Reference, Montana State University, Bozeman, Montana, 1987.

58. Wolf, S., and Tauber, R.N. "Silicon Processing for the VLSI Era: Process Technology", Lattice Press, California, p. 112-123, 1986.

59. Ohba, T.; Ohyama, Y.; Inoue, S.; Maeda, M. in "Tungsten and Other Refractory Metals for VLSI Applications II", E.K. Broadbent, Ed., MRS, Pittsburg, 1986.

60. Carlsson, J., and Boman, M. J. Vac. Sci. Tech., A, Vol. 3, No. 6, Nov/Dec 1985, p. 2298-2302.

61. Creighton, J.R. in "Tungsten and Ohter Refractory Metals for VLSI Applications II", E.K. Broadbent, Ed., MRS, Pittsburg, 1986.

62. Heller, S.R., and Milne, G.W. EPA-NIH Mass Spectral Data Base, Vol. 3 (NBS, Washington, 1978), p. 2223.